Impaired Aryl Hydrocarbon Receptor Ligand Production by the Gut Microbiota Is a Key Factor in Metabolic Syndrome

Jane Natividad, Allison Agus, Julien Planchais, Bruno Lamas, Anne
Charlotte Jarry, Rebeca Martin, Marie-Laure Michel, Caroline
Chong-Nguyen, Ronan Roussel, Marjolene Straube, et al.

Graphical Abstract

Impaired aryl hydrocarbon receptor ligands production by the gut microbiota is a key factor in metabolic syndrome

Jane M. Natividad[1,†], Allison Agus[1,†] , Julien Planchais[1], Bruno Lamas[1,2], Anne Charlotte Jarry[3], Rebeca Martin[1], Marie-Laure Michel[1], Caroline Chong-Nguyen[3], Ronan Roussel[4,5], Marjolene Straube[2], Sarah Jegou[2], Claire McQuitty[2], Maude Le Gall[3], Gregory da Costa[1], Emmanuelle Lecornet[6], Chloé Michaudel[1], Morgane Modoux[1,2], Jeremy Glodt[1], Chantal Bridonneau[1], Bruno Sovran[1], Louise Dupraz[1,2], Andre Bado[3], Mathias L. Richard[1], Philippe Langella[1], Boris Hansel[4,5], Jean-Marie Launay[7], Ramnik J Xavier[8-11], Henri Duboc[3], and Harry Sokol[1,2, 12*]

[1]Micalis Institute, Institut National de la Recherche Agronomique (INRA), AgroParisTech, Université Paris–Saclay, 78352 Jouy-en-Josas, France

[2]Sorbonne Universités, UPMC Univ. Paris 06, École normale supérieure, CNRS, INSERM, APHP Laboratoire des Biomolécules (LBM), 27 rue de Chaligny, 75012 Paris, France

[3]Inserm UMR 1149, UFR de Médecine Paris Diderot, Université Paris Diderot, Sorbonne Paris Cité, DHU Unity APHP, F-75890 Paris France

[4]Department of Endocrinology, Diabetology, Nutrition, HUPNVS, AP-HP, Paris Diderot University- Sorbonne Paris Cité, Paris, France

[5]INSERM, U-1138, Centre de Recherche des Cordeliers, Paris, France

[6]Department of Diabetology, Assistance publique-Hôpitaux de Paris (AP-HP), Pitié-Salpêtrière Hospital, 75013 Paris, France

[7]INSERM, UMR S942, Department of Biochemistry, Lariboisière Hospital, Paris, France

[8]Broad Institute of Massachusetts Institute of Technology (MIT) and Harvard University, Cambridge, Massachusetts, USA

[9]Center for Computational and Integrative Biology, Massachusetts General Hospital and Harvard Medical School, Boston, Massachusetts, USA

[10]Gastrointestinal Unit and Center for the Study of Inflammatory Bowel Disease, Massachusetts General Hospital and Harvard Medical School, Boston, Massachusetts, USA

[11]Center for Microbiome Informatics and Therapeutics, MIT, Cambridge, Massachusetts, USA

[12]Department of Gastroenterology, Saint Antoine Hospital, Assistance Publique – Hopitaux de Paris, UPMC, Paris, France

† These authors contributed equally

*Correspondence/Lead Contact:

Pr Harry Sokol

Gastroenterology Department

Hôpital Saint-Antoine

184 rue du Faubourg Saint-Antoine, 75571 Paris CEDEX 12, France

Tel.: +33 1 49 28 31 71

Fax: +33 1 49 28 31 88

harry.sokol@aphp.fr

SUMMARY

The extent by which microbiota alterations define or influence the outcome of metabolic diseases is still unclear, but the by-products of microbiota metabolism are known to have an important role in mediating the host-microbiota interaction. Here, we identify that in both pre-clinical and clinical settings, metabolic syndrome is associated with the reduced capacity of the microbiota to metabolize tryptophan into derivatives that are able to activate the aryl hydrocarbon receptor. This alteration is not merely an effect of the disease as supplementation with AhR agonist or a *Lactobacillus* strain, with a high AhR ligand-production capacity, leads to improvement of both dietary- and genetic induced metabolic impairments, particularly glucose dysmetabolism and liver steatosis, through improvement of intestinal barrier function and secretion of the incretin hormone GLP-1. These results highlight the role of gut microbiota-derived metabolites as a biomarker and as a basis for novel preventative or therapeutic interventions for metabolic disorders.

KEYWORDS: AhR, High fat diet, *L. reuteri,* microbiota, metabolites, ob/ob mice

INTRODUCTION

The mammalian gastrointestinal tract is a natural bioreactor for diverse and highly mutualistic microorganisms, collectively referred to as the gut microbiota. Disruptions of the microbiota composition and function, which are caused by factors such as genetics and lifestyle choices have been suggested to be critical contributing factors to the growth of the worldwide epidemics of chronic illness, including inflammatory and metabolic diseases (Ley et al., 2005; Ley et al., 2006a; Ridaura et al., 2013; Turnbaugh et al., 2006). The

molecular mechanisms that govern the pathogenic role of the microbiota, especially in metabolic syndrome, however, remain elusive.

The gut microbiota continually produces extremely diverse repertoire of metabolites from fermentation of both exogenous, such as dietary components, and endogenous sources (Blacher et al., 2017). These metabolites serve as important signals that contribute to the proper regulation of the host physiology and maintenance of health (Schirmer et al., 2016). As such, a need to define and characterize different microbiota-derived metabolites to complement gut microbiota compositional and functional characterization is beneficial not only to mechanistically understand the host-microbiota crosstalk but to also identify possible biomarkers or signature for health and disease.

A group of microbiota metabolites, such as those produced through metabolism of tryptophan from dietary sources, have been shown to signal through the aryl hydrocarbon receptor (AhR) (Zelante et al., 2013). AhR activation leads to several cellular responses and pathways including hormone and immune responses (Furue et al., 2014; Hao and Whitelaw, 2013; Leavy, 2011; Murray et al., 2014; Lamas et al., 2018), and thus can greatly influence health and disease risks. Indeed, we recently showed that the inefficiency of gut microbiota to produce tryptophan-based AhR ligands is involved in the pathogenesis of inflammatory bowel disease, notably through impairment of interleukin (IL)-22 production (Lamas et al., 2016). Defective intestinal production of IL-22 has similarly been observed in mice fed a high fat diet (HFD) (Wang et al., 2014), but whether impaired microbiota-derived AhR ligands contributes to metabolic disorders have not yet been fully explored.

Independently of the gut microbiota, several studies have already investigated the possible role of AhR in metabolic syndrome by comparing the evolution of diet-induced metabolic impairments in $AhR^{-/-}$ to $AhR^{+/+}$ mice. Possibly due to growth retardation observed in $AhR^{-/-}$ mice and phenotype variability between $AhR^{-/-}$ strains (Esser, 2009), the results have been contradictory, with some studies suggesting that AhR is deleterious (Korecka et al., 2016) while others suggest that AhR is protective (Wada et al., 2016) against diet-induced metabolic syndrome.

Based on the known altered gut microbiota composition and function and on the clues suggesting an abnormal AhR signaling in metabolic syndrome, we hypothesized that an impaired production of AhR agonists by the gut microbiota could play a role in metabolic syndrome pathogenesis.

Here, we identify that the fecal samples of individuals with metabolic syndrome display low levels of tryptophan-based metabolites and this is paralleled by reduced AhR activity of the fecal samples. Similar AhR ligands deficiency is observed in animal models of metabolic syndrome. Treatment with either an AhR agonist or a *Lactobacillus* strain, with a high tryptophan metabolizing capabilities, to compensate for the impaired microbiota-derived AhR ligands signaling, reduces glucose dysmetabolism and liver steatosis in animal models. Mechanistically, metabolic improvement is linked to the restoration of the intestinal barrier function and production of the intestinal incretin hormone.

Results

Impaired microbiota metabolites and AhR activity in individuals with metabolic syndrome

To study the relevance of gut microbiota-derived AhR ligands in metabolic syndrome, we analyzed the concentrations of specific microbiota metabolites known to activate AhR in the fecal samples of individuals with metabolic syndrome and healthy subjects (Table S1). Fecal samples from obese individuals (body mass index, BMI>30) showed lower concentrations of AhR agonists, including indole, indole acetic acid (IAA), 3-methyl-indole and tryptamine, compared to those from non-obese individuals (Figure 1A, Figure S1A-D). Furthermore, the abundance of AhR agonists and BMI showed a strong negative correlation (Figure 1B, Figure S1E). Individuals displaying metabolic risk factors, such as type-2 diabetes (T2D) and high blood pressure (HBP), similarly showed lower fecal concentrations of AhR ligands (Figure 1C-D). In contrast, the concentration of kynurenine, a tryptophan metabolite produced by the host cells through the enzyme indoleamine 2,3-dioxygenase 1 (IDO), which is implicated as a key contributor to the development of chronic inflammatory diseases (Prendergast et al., 2011), were significantly increased in the fecal samples of individuals with metabolic syndrome (Figure 1E-H), a result consistent with the low-grade chronic intestinal inflammation associated with metabolic disorder (Ding and Lund, 2011; Gulhane et al., 2016; Luck et al., 2015).

To investigate the functional relevance of the tryptophan-based metabolite deficiencies, we investigated the capacity of the fecal samples from individuals displaying risk factors for metabolic syndrome to activate AhR *in-vitro*. Consistent with low levels of metabolites, AhR agonist activity of fecal samples from individuals with metabolic syndrome were significantly lower compared to healthy subjects (Figure 1I-L, Figure S1F-

H). Collectively, these clinical data demonstrate an alteration of the production of microbiota-derived AhR ligands in metabolic syndrome and suggest a potential role in its pathogenesis.

Altered microbiota composition and reduced microbiota-derived AhR ligands in animal models of metabolic syndrome

To investigate the causative link between the altered production of microbiota-derived AhR ligands and metabolic syndrome pathogenesis, we used pre-clinical animal models of metabolic diseases. In line with the clinical results, the colon content of the HFD-fed mice, which displayed features of metabolic disorders including glucose intolerance and hepatic steatosis (Figure S2 A-K), showed decreased AhR agonist activity and lower concentrations of microbiota-derived AhR ligands in the colon content compared with that of conventional diet (CD)-fed mice (Figure 2A-D). Additionally, similar to previous reports (Wang et al., 2014), HFD-fed mice displayed lower intestinal expression of *Il22, Reg3g* and *Reg3b* which are AhR target genes (Figure 2E-G). Total tryptophan concentration was significantly lower in the colon of HFD compared to CD (Figure 2H). On the other hand, IDO activity and the concentration of kynurenine were significantly increased in the colon content of HFD group (Figure 2I-J).

The decreased AhR metabolic activity of the HFD microbiota was associated with a different profile from that of the CD microbiota (Figure 2K) but no difference in total bacterial abundance was observed (Figure S2L). Specifically, the HFD microbiota showed a relative increase in bacteria belonging to the Lachnospiraceae and Clostridiaceae families and to Proteobacteria phylum, whereas there was a lower abundance of bacteria from the

Rikenellaceae and Bifidobacteriaceae families and of *Akkermansia muciniphila* than that in the CD microbiota (Figure 2L-M).

To specifically demonstrate that the altered microbiota composition and/or function is causal in the defective production of AhR agonists, we performed a fecal microbiota transplantation experiment. Germ-free mice fed a conventional diet were colonized with the fecal microbiota of either CD-fed or HFD-fed mice. AhR activity in stool assessed 3 weeks later showed a significantly lower level in mice colonized with HFD-fed microbiota demonstrating a causal effect of microbiota alterations in the decreased production of AhR agonists (Figure S2M).

Finally, lower AhR activity was similarly observed in the colon contents of HFD-fed rats and in a murine model of genetically induced metabolic disorder (leptin-deficient, ob/ob mice) (Figure 2N-O), although the bacterial composition was different in HFD-fed and ob/ob mice (Figure S2N). These results demonstrate that reduced production of microbiota-derived AhR ligands is a trans-species signature profile of metabolic disease.

Treatment with AhR agonist reduced features of HFD-induced metabolic syndrome

To investigate the physiological importance of impaired microbiota AhR activity, 6-formylindolo(3,2-b)carbazole (Ficz), an AhR agonist, was administered to HFD-fed mice. The Ficz treatment did not significantly affect weight gain (Figure S6A), but it did improve glucose metabolism, as observed through a homeostatic model assessment-insulin resistance method (HOMA-IR), in the HFD group (Figure 3A, Figure S6B-C). HFD-fed mice also showed better glucose clearance during the oral glucose tolerance test (OGTT) and higher insulin sensitivity during the insulin tolerance test (ITT) (Figure 3B-E).

Improved features of fatty liver, characterized by lower hepatic triglycerides and lower serum concentrations of liver-specific enzyme alanine transaminase (ALT) but not aspartate aminotransferase (AST) were observed in Ficz-treated mice (Figure 3F-I, Figure S6D). Finally, lower levels of plasma cholesterol were also observed in Ficz-treated mice compared to non-treated (Figure 3J).

Ficz was unable to correct the impaired AhR agonist production of the microbiota or the microbiota composition (Figure 3K-L) but was sufficient to restore intestinal expression of *Cyp1a1 and Il-22* , which are target genes of AhR activation (Figure S7), thus highlighting the efficacy of the Ficz treatment in compensating for the decreased microbiota-specific AhR signaling. The AhR-dependent mechanism of Ficz was confirmed by its lack of efficacy in treating metabolic syndrome in HFD-fed *AhR*$^{-/-}$ mice (Figure S4).

Treatment with AhR agonist reduced features of genetic-induced metabolic syndrome

We further investigated the therapeutic value of Ficz in the leptin deficent ob/ob mice, a mutant mice strain that profoundly develop metabolic syndrome due to excessive eating. Similar to HFD, Ficz did not significantly affect weight gain in ob/ob mice (Figure S5A). However, Ficz treated *ob/ob* mice showed significantly lower fasting glucose than non-treated ones (Figure 4A) but no difference was observed for fasting insulin and HOMA-IR (Figure S5B-C). Fasting glucose was similar between WT and ob/ob mice but fasting insulin was dramatically higher in ob/ob suggesting that at this stage, hyperglycemia is still controlled by over production of insulin. Furthermore, Ficz treatment was efficient in decreasing glucose and insulin dysmetabolism in ob/ob mice, as assessed by OGTT and ITT respectively (Figure 4B-E). Ficz treated *ob/ob* mice further displayed

reduced features of hepatic dysfunction, characterized by lower hepatic lipids and lower serum ALT but not AST (Figure 4F-I, S5D). Moreover, serum triglyceride levels were significantly reduce in Ficz treated ob/ob mice (Figure 4J). Taken together, these results demonstrate that AhR agonist Ficz has therapeutic effect in both HFD- and genetic-induced metabolic syndrome.

Supplementation with L. reuteri that highly produce AhR ligands improves metabolic syndrome

We next investigated whether administration of a previously isolated *Lactobacilllus reuteri* strain that naturally exhibits high AhR-ligand production (Lamas et al., 2016) can similarly reverse the diet-associated metabolic dysfunction. *L. reuteri* supplementation was sufficient to rescue the impaired AhR activity of the gut microbiota of HFD-fed mice (Figure 5A). *L. reuteri* treatment did not significantly affect weight in all groups (Figure S5E) but it recapitulated the improvements demonstrated by Ficz treatment. In particular, *L. reuteri*-supplemented HFD mice showed improved HOMA-IR, glucose clearance and better insulin sensitivity than non-supplemented mice (Figure 5B-F). Furthermore, HFD-*L. reuteri* group displayed lower fasting insulin level but not fasting glucose (Figure S5F-G). HFD-*L. reuteri* also showed improved liver histology as well as lower levels of hepatic triglycerides and serum ALT and triglcyerides levels but not AST (Figure 5G-J; Figure S5H). When administered in AhR$^{-/-}$ mice in HFD context, the *L. reuteri* strain did not exhibit beneficial effects on glucose clearance during OGTT test (Figure S6A and B) and on steatosis (Figure S6C and D), showing that one of the major mechanism of action of this strain is AhR-dependent. Finally, another *Lactobacillus* strain

that does not exhibit AhR-ligand production (Figure S6E), did not have any beneficial effects on glucose clearance during OGTT test (Figure S6F and G) and on steatosis (Figure S6H and I). Overall, this underscores that microbiota-specific AhR activation is instrumental in the maintenance of metabolic homeostasis.

Restoration of AhR activity improved intestinal barrier function in animal model of metabolic syndrome

We next explored the potential mechanisms of action underlying the positive effect of the restoration of AhR activity in metabolic syndrome. Intestinal barrier dysfunction and low-grade inflammation have been widely accepted as distinctive features of metabolic disorders. Hence, we next determined whether activation of AhR signaling affects intestinal barrier function by evaluating the permeability of different intestinal segments using an Ussing chamber system. Similarly to findings from previous studies reporting barrier dysfunction in HFD-fed animals (Johnson et al., 2015), we found that the HFD-fed mice showed higher translocation of fluorescein-labeled LPS (F-LPS) and other permeability markers, namely, fluorescein-labeled sulfonic acid (FS4) and antonia-red-labeled dextran (ARD4), than did the CD-fed mice, particularly in the colon and jejunum (Figure 6A, Figure S7). The Ficz treatment was effective in decreasing the barrier dysfunction in the HFD-fed mice (Figure 6A).

To confirm whether the barrier improvement was specific to Ficz signaling, we used a reductionist system involving a human intestinal epithelial cell line. Ficz stimulation prevented the TNF-α-induced decrease in trans-epithelial electric resistance (TEER) and increased translocation of fluorescein-labeled dextran (FD4) *in vitro* (Figure 6B-C).

We next determined the relevance of increased permeability in HFD-fed mice by measuring the serum concentration of soluble CD14 (sCD14), which is released from monocytes after LPS activation and is thus used as a surrogate marker for systemic LPS availability. The HFD-fed mice, compared with the CD-fed mice, showed elevated levels of serum sCD14, and the Ficz treatment in the HFD-fed mice significantly prevented the serum sCD14 elevation (Figure 6D). In addition, the Ficz-treated HFD mice, as compared with the untreated mice, showed decreased levels of systemic inflammatory markers, which were characterized by decreased TNF-α and IFN-γ production by splenic cells (Figure 6E-F). Globally, these results show that the beneficial effects of AhR agonist involve the correction of the intestinal barrier defect associated with metabolic syndrome.

AhR ligand induced the secretion of the incretin hormone GLP-1

Beside their effects on intestinal barrier function, AhR agonists might have other targets in the gut explaining their beneficial effects in metabolic syndrome. Microbiota-derived indole has been shown to be efficient in stimulating the secretion of the incretin hormone GLP-1 from intestinal enteroendocrine cells (EECs) (Chimerel et al., 2014) but a potential link with AhR has not been investigated. In accordance with findings from previous reports (Richards et al., 2016), we observed significantly lower expression of intestinal *proglucagon (Gcg)*, which encodes GLP-1, and decreased levels of total GLP-1 in the plasma of HFD-fed mice than in the plasma of CD-fed mice (Figure 7A-B). The Ficz treatment restored intestinal mRNA expression of *Gcg* and plasma GLP-1 levels in the HFD-fed mice.

To explore whether AhR agonists directly stimulate the production of GLP-1, the GLUTag cell line, which is a murine EEC line that expresses the *Gcg* gene, secretes GLP-1 (Drucker et al., 1994) as well as expresses AhR, was stimulated with Ficz. Ficz promoted strong GLP-1 secretion to levels comparable to that observed when GLUTag cells were stimulated with Forskolin, a strong inducer of GLP-1 secretion that acts through G protein-coupled receptors (Lan et al., 2012). This effect was AhR specific, because the response disappeared in the presence of an AhR antagonist (Figure 7C). Together, these data show a novel mechanism by which microbiota-dependent AhR signaling may contribute to the outcome of metabolic dysfunction through modulation of GLP-1 production.

Discussion

Metabolic syndrome and its associated conditions, such as obesity, T2D and non-alcoholic fatty liver disease, are major health concerns worldwide (Sonnenburg and Backhed, 2016). Compositional microbiota alterations have been described in metabolic disorders (Ley et al., 2005; Ley et al., 2006a; Ridaura et al., 2013; Turnbaugh et al., 2006) but the functional alteration of the gut microbiota and their role in disease pathogenesis remain poorly defined.

The microbiota-derived tryptophan metabolites, such as indole, which are ligands for AhR, have a major role in intestinal homeostasis (Lamas et al., 2018) and have been implicated in pathogenesis of inflammatory bowel disease (Lamas et al., 2016). Several reports suggested a possible role of AhR in metabolic syndrome pathogenesis and an altered activation of AhR target genes has been observed in the gut of mice with metabolic syndrome (Wang et al., 2014). Here, we asked whether the production of AhR agonists by

the gut microbiota is altered in metabolic syndrome and if it has a role in the disease pathogenesis.

We show that the microbiota of humans with metabolic syndrome and of animal models of metabolic syndrome exhibit an impaired AhR agonist activity, which was consistent with lower AhR ligand concentrations. Changes in microbiota-derived AhR ligands was associated with shifts in microbiota composition, a result reminiscent of previous reports showing that the microbiota of obese humans and animals contain higher levels of Firmicutes and lower levels of Bacteroidetes (Ley et al., 2005; Ley et al., 2006b). Whilst these results highlight the importance of both the composition and function of the microbiota, the causal relevance of these changes remained contentious. Hence, using diet and genetic-induced animal models of metabolic syndrome, we explored the crosstalk between AhR and microbiota metabolites in the regulation of metabolic function.

AhR activation leads to myriad of cellular pathways including IL-22 signaling, which have been shown to alleviate metabolic disorders (Wang et al., 2014). Due to contradictory results from studies using either mice that lacks AhR or AhR antagonist, doubts about the specific involvement of AhR in metabolic diseases have been casted. AhR is widely distributed on different cell types in mammalian body, both in systemic and mucosal compartment, and is able to responds to different ligands with varying structure and physiochemical properties; thus, the effect of AhR signaling may be dependent on the targeted organ, on the differences in AhR ligand-binding capacity and downstream activities. The aim of our study was to elucidate the specific contribution of microbiota-derived AhR ligands in modulating metabolic diseases. Thus, to avoid these pitfalls and in

accordance with our specific question, we employed a strategy that involves compensating the deficiency in microbiota-derived AhR signaling.

To fully understand the system, we chose to supplement the animal models with interventions that have two different way of compensation. In particular, *L. reuteri* compensates for impaired AhR signaling by increasing the availability of intestinal metabolites able to signal through AhR, while Ficz directly signals through AhR. Both interventions effectively improve metabolic impairments, and underscore that microbiota-specific AhR activation is instrumental in the maintenance of metabolic homeostasis.

Intestinal barrier dysfunction and low-grade inflammation are distinctive features of metabolic diseases (Everard and Cani, 2013). A leaky gut permits the passage of microbial products, such as lipopolysaccharide (LPS), across the mucosa. This passage causes metabolic endotoxemia, which manifests as a moderate increase in the plasma LPS concentration. This phenotype is observed in humans and animals with metabolic syndrome and has been shown to trigger the systemic inflammatory reaction that drives metabolic disease (Cani et al., 2007; Cani et al., 2008; Shi et al., 2006). In light of these data, we sought to determine whether activation of AhR signaling in the gut affects intestinal barrier function by evaluating the intestinal permeability. The Ficz treatment was efficient in correcting the barrier dysfunction as well as subsequent systemic LPS bioavailability and inflammation in HFD-fed mice. Similar studies have demonstrated the efficacy of Ficz in reversing hypoxia-driven intestinal barrier dysfunction (Han et al., 2016) and the importance of AhR ligands, especially bacteria-derived indole metabolites, in regulating mucosal and epithelial barrier integrity (Li et al., 2011; Qiu et al., 2012; Venkatesh et al., 2014; Zelante et al., 2013). Thus, together with our results, these data

highlight the beneficial effect of AhR signaling at the epithelial cell level. Interestingly, it has been recently shown that *L. reuteri* is able to reprogram intraepithelial CD4$^+$ T cells into immunoregulatory T cells in an AhR-dependent manner (Cervantes-Barragan et al., 2017), suggesting another possible mechanism for improvement of intestinal barrier integrity in metabolic syndrome context.

We further showed that AhR signaling is able to induce the secretion of the incretin hormone GLP-1 from intestinal enteroendocrine cells (EECs). GLP-1 has myriad metabolic functions, including roles in glucose homeostasis and liver function, and drugs that mimic GLP-1 actions are now widely used to treat T2D. Overall, our data show a novel mechanism by which microbiota-dependent AhR signaling may contribute to the outcome of metabolic dysfunction. Our results do not allow to determine whether the alteration of AhR agonists production by the gut microbiota is primary event in metabolic syndrome pathogenesis. However, the therapeutic effect of the correction of this defect clearly shows its involvement in the pathogenesis. One possible explanation could be that early events in metabolic syndrome pathogenesis lead to alterations of gut microbiota composition and function and notably to a decreased production of AhR agonists, that itself favors the worsening of metabolic syndrome in a kind of vicious circle.

In summary, our study identified a new mechanism linking the gut microbiota to metabolic syndrome. The decreased ability of the microbiota to produce AhR ligands leads to defective mucosal barrier integrity and reduced GLP-1 secretion, and ultimately facilitates the development of more severe metabolic syndrome. Importantly, these results are relevant to humans, because impaired AhR agonist activity is similarly observed in patients with metabolic syndrome. In addition to providing key evidence of the importance

of the microbiota composition and function in the maintenance of host metabolic homeostasis, this study lays the groundwork for further studies aiming to pharmacologically correct the AhR ligand deficiency in metabolic disorders by using techniques such as supplementation with natural AhR ligand-producing bacteria. In conclusion, our data pave the way for new preventive or curative treatments of metabolic syndrome.

Limitation of the study

The defect in AhR agonist production by the gut microbiota in metabolic syndrome was observed in humans and was confirmed in both rats and mice. However, all the experiments evaluating the effects of correcting this defect were carried out in mice, which can be seen as a potential limitation. Further interventional studies in human should be done in the future to evaluate the proposed therapeutic strategy.

AUTHOR CONTRIBUTIONS

J.M.N., A.A. and H.S. conceptualized and designed the study and performed the data analysis. J.M.N. and A.A. conducted all experiments, unless otherwise indicated. B.L., R.M., M-L.M., M.S., S.J., G.dG., C.B., B.S., J.P., and M.L-R. provided technical assistance for the *in vitro* and *in vivo* experiments. M.L.G., A.C.J., A.B., and H.D. performed experiments with the ob/ob mice and rats. H.S., C.C.-N., R.R., C.M., E.L., B.H., J-M.L., and H.D. provided the human clinical data and samples. J.M.N, R.J.X., P.L., H.D., A.B., E.L., M.L.G. and H.S. discussed the experiments and results. J.M.N, A.A and H.S wrote the manuscript.

DECLARATION OF INTERESTS

Patents related to this work : EP 15306303.7 ; EP16306300.1

HS and PL are co-founder of Nextbiotix. JMN is currently an employee of Nestlé.

REFERENCE

Blacher, E., Levy, M., Tatirovsky, E., Elinav, E. (2017). Microbiome-Modulated Metabolites at the Interface of Host Immunity. J Immunol *198*,572-580.

Cani, P.D., Amar, J., Iglesias, M.A., Poggi, M., Knauf, C., Bastelica, D., Neyrinck, A.M., Fava, F., Tuohy, K.M., Chabo, C., et al. (2007). Metabolic endotoxemia initiates obesity and insulin resistance. Diabetes *56*, 1761-1772.

Cani, P.D., Bibiloni, R., Knauf, C., Waget, A., Neyrinck, A.M., Delzenne, N.M., and Burcelin, R. (2008). Changes in gut microbiota control metabolic endotoxemia-induced

inflammation in high-fat diet-induced obesity and diabetes in mice. Diabetes *57*, 1470-1481.

Cervantes-Barragan, L., Chai, J.N., Tianero, M.D., Di Luccia, B., Ahern, P.P., Merriman, J., Cortez, V.S., Caparon, M.G., Donia, M.S., Gilfillan, S., et al. (2017). Lactobacillus reuteri induces gut intraepithelial CD4(+)CD8αα(+) T cells. Science *6353*, 806-810.

Chimerel, C., Emery, E., Summers, D.K., Keyser, U., Gribble, F.M., and Reimann, F. (2014). Bacterial metabolite indole modulates incretin secretion from intestinal enteroendocrine L cells. Cell reports *9*, 1202-1208.

Crane, J.D., Palanivel, R., Mottillo, E.P., Bujak, A.L., Wang, H., Ford, R.J., Collins, A., Blumer, R.M., Fullerton, M.D., Yabut, J.M., et al. (2015). Inhibiting peripheral serotonin synthesis reduces obesity and metabolic dysfunction by promoting brown adipose tissue thermogenesis. Nat Med *21*, 166-172.

Ding, S., and Lund, P.K. (2011). Role of intestinal inflammation as an early event in obesity and insulin resistance. Curr Opin Clin Nutr Metab Care *14*, 328-333.

Drucker, D.J., Jin, T., Asa, S.L., Young, T.A., and Brubaker, P.L. (1994). Activation of proglucagon gene transcription by protein kinase-A in a novel mouse enteroendocrine cell line. Mol Endocrinol *8*, 1646-1655.

Edgar, R.C. (2010). Search and clustering orders of magnitude faster than BLAST. Bioinformatics *26*, 2460-2461.

Esser, C. (2009). The immune phenotype of AhR null mouse mutants: not a simple mirror of xenobiotic receptor over-activation. Biochem Pharmacol *77*, 597-607.

Everard, A., and Cani, P.D. (2013). Diabetes, obesity and gut microbiota. Best practice & research. Clinical gastroenterology *27*, 73-83.

Furue, M., Takahara, M., Nakahara, T., and Uchi, H. (2014). Role of AhR/ARNT system in skin homeostasis. Arch Dermatol Res *306*, 769-779.

Garner, C.E., Smith, S., de Lacy Costello, B., White, P., Spencer, R., Probert, C.S., and Ratcliffe, N.M. (2007). Volatile organic compounds from feces and their potential for diagnosis of gastrointestinal disease. FASEB J *21*, 1675-1688.

Gulhane, M., Murray, L., Lourie, R., Tong, H., Sheng, Y.H., Wang, R., Kang, A., Schreiber, V., Wong, K.Y., Magor, G., et al. (2016). High Fat Diets Induce Colonic Epithelial Cell Stress and Inflammation that is Reversed by IL-22. Scientific reports *6*, 28990.

Han, B., Sheng, B., Zhang, Z., Pu, A., Yin, J., Wang, Q., Yang, K., Sun, L., Yu, M., Qiu, Y., et al. (2016). Aryl Hydrocarbon Receptor Activation in Intestinal Obstruction Ameliorates Intestinal Barrier Dysfunction Via Suppression of MLCK-MLC Phosphorylation Pathway. Shock *46*, 319-328.

Hao, N., and Whitelaw, M.L. (2013). The emerging roles of AhR in physiology and immunity. Biochem Pharmacol *86*, 561-570.

Johnson, A.M., Costanzo, A., Gareau, M.G., Armando, A.M., Quehenberger, O., Jameson, J.M., and Olefsky, J.M. (2015). High fat diet causes depletion of intestinal eosinophils associated with intestinal permeability. PLoS One *10*, e0122195.

Korecka, A., Dona, A., Lahiri, S., Tett, A.J., Al-Asmakh, M., Braniste, V., D'Arienzo, R., Abbaspour, A., Reichardt, N., Fujii-Kuriyama, Y., et al. (2016). Bidirectional communication between the Aryl hydrocarbon Receptor (AhR) and the microbiome tunes host metabolism. NPJ biofilms and microbiomes *2*, 16014.

Lahvis, G.P., and Bradfield, C.A. (1998). Ahr null alleles: distinctive or different? Biochem Pharmacol *56*, 781-787.

Lamas, B., Richard, M.L., Leducq, V., Pham, H.P., Michel, M.L., Da Costa, G., Bridonneau, C., Jegou, S., Hoffmann, T.W., Natividad, J.M., et al. (2016). CARD9 impacts colitis by altering gut microbiota metabolism of tryptophan into aryl hydrocarbon receptor ligands. Nat Med *22*, 598-605.

Lamas, B., Natividad, J.M., Sokol H. (2018). Aryl hydrocarbon receptor and intestinal immunity. Mucosal Immunol. 2018 Apr 7.

Lan, H., Lin, H.V., Wang, C.F., Wright, M.J., Xu, S., Kang, L., Juhl, K., Hedrick, J.A., and Kowalski, T.J. (2012). Agonists at GPR119 mediate secretion of GLP-1 from mouse enteroendocrine cells through glucose-independent pathways. Br J Pharmacol *165*, 2799-2807.

Laval, L., Martin, R., Natividad, J.N., Chain, F., Miquel, S., Desclee de Maredsous, C., Capronnier, S., Sokol, H., Verdu, E.F., van Hylckama Vlieg, J.E., et al. (2015).

Lactobacillus rhamnosus CNCM I-3690 and the commensal bacterium Faecalibacterium prausnitzii A2-165 exhibit similar protective effects to induced barrier hyper-permeability in mice. Gut microbes *6*, 1-9.

Leavy, O. (2011). Mucosal immunology: the 'AHR diet' for mucosal homeostasis. Nat Rev Immunol *11*, 806.

Ley, R.E., Backhed, F., Turnbaugh, P., Lozupone, C.A., Knight, R.D., and Gordon, J.I. (2005). Obesity alters gut microbial ecology. Proc Natl Acad Sci U S A *102*, 11070-11075.

Ley, R.E., Turnbaugh, P.J., Klein, S., and Gordon, J.I. (2006a). Microbial ecology: human gut microbes associated with obesity. Nature *444*, 1022-1023.

Ley, R.E., Turnbaugh, P.J., Klein, S., and Gordon, J.I. (2006b). Microbial ecology: human gut microbes associated with obesity. Nature *444*, 1022-1023.

Li, Y., Innocentin, S., Withers, D.R., Roberts, N.A., Gallagher, A.R., Grigorieva, E.F., Wilhelm, C., and Veldhoen, M. (2011). Exogenous stimuli maintain intraepithelial lymphocytes via aryl hydrocarbon receptor activation. Cell *147*, 629-640.

Luck, H., Tsai, S., Chung, J., Clemente-Casares, X., Ghazarian, M., Revelo, X.S., Lei, H., Luk, C.T., Shi, S.Y., Surendra, A., et al. (2015). Regulation of obesity-related insulin resistance with gut anti-inflammatory agents. Cell Metab *21*, 527-542.

McDonald, D., Price, M.N., Goodrich, J., Nawrocki, E.P., DeSantis, T.Z., Probst, A., Andersen, G.L., Knight, R., and Hugenholtz, P. (2012). An improved Greengenes taxonomy with explicit ranks for ecological and evolutionary analyses of bacteria and archaea. ISME J *6*, 610-618.

Moyer, B.J., Rojas, I.Y., Kerley-Hamilton, J.S., Nemani, K.V., Trask, H.W., Ringelberg, C.S., Gimi, B., Demidenko, E., and Tomlinson, C.R. (2017). Obesity and fatty liver are prevented by inhibition of the aryl hydrocarbon receptor in both female and male mice. Nutrition research *44*, 38-50.

Murray, I.A., Patterson, A.D., and Perdew, G.H. (2014). Aryl hydrocarbon receptor ligands in cancer: friend and foe. Nat Rev Cancer *14*, 801-814.

Prendergast, G.C., Chang, M.Y., Mandik-Nayak, L., Metz, R., and Muller, A.J. (2011). Indoleamine 2,3-dioxygenase as a modifier of pathogenic inflammation in cancer and other inflammation-associated diseases. Curr Med Chem *18*, 2257-2262.

Qiu, J., Heller, J.J., Guo, X., Chen, Z.M., Fish, K., Fu, Y.X., and Zhou, L. (2012). The aryl hydrocarbon receptor regulates gut immunity through modulation of innate lymphoid cells. Immunity *36*, 92-104.

Richards, P., Pais, R., Habib, A.M., Brighton, C.A., Yeo, G.S., Reimann, F., and Gribble, F.M. (2016). High fat diet impairs the function of glucagon-like peptide-1 producing L-cells. Peptides *77*, 21-27.

Ridaura, V.K., Faith, J.J., Rey, F.E., Cheng, J., Duncan, A.E., Kau, A.L., Griffin, N.W., Lombard, V., Henrissat, B., Bain, J.R., et al. (2013). Gut microbiota from twins discordant for obesity modulate metabolism in mice. Science *341*, 1241214.

Schirmer, M., Smeekens, S.P., Vlamakis, H., Jaeger, M., Oosting, M., Franzosa, E.A., Jansen, T., Jacobs, L., Bonder, M.J., Kurilshikov, A., et al. (2016). Linking the Human Gut Microbiome to Inflammatory Cytokine Production Capacity. Cell *167*, 1125-1136 e1128.

Schmieder, R., and Edwards, R. (2011). Quality control and preprocessing of metagenomic datasets. Bioinformatics *27*, 863-864.

Schneider, C.A., Rasband, W.S., and Eliceiri, K.W. (2012). NIH Image to ImageJ: 25 years of image analysis. Nat Methods *9*, 671-675.

Segata, N., Izard, J., Waldron, L., Gevers, D., Miropolsky, L., Garrett, W.S., and Huttenhower, C. (2011). Metagenomic biomarker discovery and explanation. Genome biology *12*, R60.

Shi, H., Kokoeva, M.V., Inouye, K., Tzameli, I., Yin, H., and Flier, J.S. (2006). TLR4 links innate immunity and fatty acid-induced insulin resistance. J Clin Invest *116*, 3015-3025.

Sonnenburg, J.L., and Backhed, F. (2016). Diet-microbiota interactions as moderators of human metabolism. Nature *535*, 56-64.

Turnbaugh, P.J., Ley, R.E., Mahowald, M.A., Magrini, V., Mardis, E.R., and Gordon, J.I. (2006). An obesity-associated gut microbiome with increased capacity for energy harvest. Nature *444*, 1027-1031.

Venkatesh, M., Mukherjee, S., Wang, H., Li, H., Sun, K., Benechet, A.P., Qiu, Z., Maher, L., Redinbo, M.R., Phillips, R.S., et al. (2014). Symbiotic bacterial metabolites regulate gastrointestinal barrier function via the xenobiotic sensor PXR and Toll-like receptor 4. Immunity *41*, 296-310.

Wada, T., Sunaga, H., Miyata, K., Shirasaki, H., Uchiyama, Y., and Shimba, S. (2016). Aryl Hydrocarbon Receptor Plays Protective Roles against High Fat Diet (HFD)-induced Hepatic Steatosis and the Subsequent Lipotoxicity via Direct Transcriptional Regulation of Socs3 Gene Expression. J Biol Chem *291*, 7004-7016.

Wang, X., Ota, N., Manzanillo, P., Kates, L., Zavala-Solorio, J., Eidenschenk, C., Zhang, J., Lesch, J., Lee, W.P., Ross, J., et al. (2014). Interleukin-22 alleviates metabolic disorders and restores mucosal immunity in diabetes. Nature *514*, 237-241.

Zelante, T., Iannitti, R.G., Cunha, C., De Luca, A., Giovannini, G., Pieraccini, G., Zecchi, R., D'Angelo, C., Massi-Benedetti, C., Fallarino, F., et al. (2013). Tryptophan catabolites from microbiota engage aryl hydrocarbon receptor and balance mucosal reactivity via interleukin-22. Immunity *39*, 372-385.

Zhang, S., Qin, C., and Safe, S.H. (2003). Flavonoids as aryl hydrocarbon receptor agonists/antagonists: effects of structure and cell context. Environmental health perspectives *111*, 1877-1882.

FIGURE LEGENDS

Figure 1. The microbiota of individuals with metabolic syndrome show decreased AhR activation and lower AhR agonist concentrations. (A) Total concentrations of 4 AhR agonists (IAA, indole, 3-methylindole and tryptamine) from feces of individuals with low and high BMIs. (B) Spearman correlation of the stool AhR agonist concentration and BMI. (C-D) AhR agonist concentrations of the feces according to T2D and high blood pressure (HBP) status. (E) Kynurenine concentrations of the feces from individuals with low and high BMIs. (F) Spearman correlation of the stool kynurenine concentration and BMI. (G-H) Kynurenine concentrations of the feces according to T2D and HBP status. (I) Quantification of the fecal AhR activity of individuals with low and high BMIs. (J) Spearman correlation of stool AhR activation and BMI. (K-L) Quantification of the fecal AhR activity according to T2D and HBP status. For AhR reporter assay, data was available in the whole population (n=127). For AhR agonist dosage, results were not available in 4 patients (3 with BMI>30 and 1 with BMI<30). For all data, statistical comparisons were carried out by normality testing using Kolmogorov-Smirnov tests and subsequent ANOVAs or Kruskal-Wallis tests with Bonferroni or Dunn's *post hoc* tests.

Figure 2. High fat diet-induced metabolic syndrome is associated with an altered microbiota composition and impaired microbiota-driven AhR activation. (A) Quantification of the fecal AhR agonist activity of mice fed a CD or HFD for 12 weeks. Fecal concentration of (B) IAA, (C) indole and (D) tryptamine in the indicated mice. Transcript expression of (E) *Il22,* (F) *Reg3g* and (G) *Reg3b* in the intestines of CD- and HFD-fed mice (*p<0.05, n=5-6/group). Quantification of (H) Tryptophan concentration, (I) IDO activity and (J) kynurenine concentration in the colon mucosa of CD- and HFD-

fed mice. (K) Principal coordinate analysis (PCoA) plot of Bray Curtis distances of the fecal microbiota of the CD-fed or HFD-fed mice (Anosim test, 9999 permutations). (L) Fecal bacterial proportion at phylum level. (M) Discriminant analysis (LEFSE) of the fecal microbiota between the CD and HFD groups. (N) Quantification of the fecal AhR agonist activity of rats fed a CD or HFD for 12 weeks. (O) Quantification of the fecal AhR activity of ob/ob and wild-type (WT) mice fed a CD at 6 weeks of age. For A-J and N-O, statistical comparisons were carried out by normality testing using the Kolmogorov-Smirnov test and subsequent unpaired t-tests or Mann-Whitney tests t-test.

Figure 3. Treatment with an AhR agonist alleviates diet-induced metabolic impairments. (A) The fasting homeostatic model assessment of insulin resistance (HOMA-IR) of CD- and HFD-fed mice treated with Ficz or vehicle (DMSO). (B) Blood glucose level before and after the oral glucose tolerance challenge of CD- and HFD-fed mice treated with Ficz or vehicle (OGTT, comparison vs HFD, n=12-20/group). (C) AUC of the OGGT. (D) Blood glucose levels before and after the ITTs (comparison vs HFD, n=6-10/group). (E) AUC of the ITT. (F) Lipid area, calculated as the % area of interest (AOI), in the liver cross-sections of CD- and HFD-fed mice treated with Ficz or vehicle. (G) Representative pictures of hematoxylin and eosin (H&E)–stained liver sections from CD- and HFD-fed mice treated with Ficz or vehicle. (H) Liver triglycerides after 6h of food deprivation. Concentrations of (I) alanine transaminase (ALT) and (J) total cholesterol from the sera of indicated mice. (K) The AhR activity of stools from mice fed a CD or HFD for 12 weeks and treated with AhR agonist Ficz or vehicle. (L) Principal coordinate analysis (PCoA) plot of Bray Curtis distances of the fecal microbiota of the CD-fed or

HFD-fed mice and treated with AhR agonist Ficz or vehicle (Anosim test, 9999 permutations). For all data, statistical comparisons were carried out by normality testing using the Kolmogorov-Smirnov test and subsequent ANOVAs or Kruskal-Wallis tests with Bonferroni or Dunn's *post hoc* tests (*$p<0.05$,**$p<0.01$, ***$p<0.001$).

Figure 4. Treatment with an AhR agonist alleviates genetic-induced metabolic impairments. (A) Blood glucose level after 6h of fasting in wild-type (WT) and *ob/ob* mice treated with Ficz or vehicle. (B) Blood glucose level before and after the oral glucose tolerance challenge of *ob/ob* mice treated with Ficz or vehicle (n=14-15/group). (C) AUC of the OGGT. (D) Blood glucose levels before and after the ITTs (n=7-8/group). (E) AUC of the ITT. (F) Lipid area, calculated as the % area of interest (AOI), in the liver cross-sections of CD- and HFD-fed mice treated with Ficz or vehicle. (G) Representative pictures of hematoxylin and eosin (H&E)–stained liver sections from indicated mice. (H) Liver triglycerides after 6h of food deprivation. Concentrations of (I) alanine transaminase (ALT) and (J) total triglycerides from the sera of indicated mice. For all data, statistical comparisons were carried out by normality testing using the Kolmogorov-Smirnov test and subsequent ANOVAs or Kruskal-Wallis tests with Bonferroni or Dunn's *post hoc* tests (*$p<0.05$,**$p<0.01$, ***$p<0.001$).

Figure 5. Supplementation with high AhR ligand-producing bacteria alleviates diet-induced metabolic impairments. (A) Quantification of the fecal AhR agonist activity of mice fed CD or HFD supplemented with *L. reuteri* or vehicle. (B) The fasting HOMA-IR of CD- and HFD-fed mice supplemented with *L. reuteri* or vehicle. (C) Blood glucose

levels before and after the OGTTs of CD- and HFD-fed mice supplemented with *L. reuteri* or vehicle (n=8/group). (D) AUC of the OGTT. (E) Blood glucose levels before and after the ITTs (n=7-8/group). (F) AUC of ITT. (G) Lipid area in the liver cross-sections of CD- and HFD-fed mice supplemented with *L. reuteri* or vehicle. (H) Representative pictures of H&E–stained liver sections from CD- and HFD-fed mice supplemented with *L. reuteri* or vehicle. Concentrations of (I) alanine transaminase (ALT) and (J) triglycerides in the sera of indicated mice. For all data, statistical comparisons were carried out by normality testing using the Kolmogorov-Smirnov test and subsequent ANOVAs or Kruskal-Wallis tests with Bonferroni or Dunn's *post hoc* tests (*$p<0.05$,**$p<0.01$, ***$p<0.001$).

Figure 6. Treatment with an AhR agonist improves HFD-induced intestinal barrier dysfunction and restores impaired incretin secretion. (A) Translocation of LPS in different intestinal tissues mounted in an Ussing chamber (n=6-12/group). (B) TEER of Caco-2 cells treated with TNF-α or vehicle in the presence of Ficz or vehicle. (C) Translocation of FD4 (fluorescein conjugated dextran) across intestinal epithelial cell monoloyer *in-vitro*. (D) Serum concentrations of soluble CD14 (sCD14) of indicated mice. (E) TNF-α and (F) IFN-γ production by spleen cells after stimulation with PMA and ionomycin. For all data, statistical comparisons were carried out by first testing normality using Kolmogorov-Smirnov tests and then performing ANOVAs or Kruskal-Wallis tests with Bonferroni or Dunn's *post hoc* tests.

Figure 7. Treatment with an AhR agonist promotes intestinal incretin secretion. (A) Expression of *Gcg* in different intestinal segments of the indicated mice (n=6-8/group). (B)

Serum concentrations of the total GLP-1 of indicated mice. (C) Quantification of GLP-1 secretion by GLUTag cells after stimulation with Ficz and Forskolin (positive control) in the presence or absence of the AhR antagonist (CH223191). For all data, statistical comparisons were carried out by first testing normality using Kolmogorov-Smirnov tests and then performing ANOVAs or Kruskal-Wallis tests with Bonferroni or Dunn's *post hoc* tests.

STAR METHODS

CONTACT FOR REAGENT AND RESOURCE SHARING

Furthermore information and requests for reagents may be directed to and will be fulfilled by the Lead Contact, Harry Sokol (harry.sokol@aphp.fr).

EXPERIMENTAL MODEL ANS SUBJECT DETAILS

Mice. Male C57BL/6JRj mice and ob/ob mice on the C57BL/6JRj background were purchased from Janvier (France) and used 1 week after receipt. $AhR^{-/-}$ mice were obtained from the Jackson laboratory (JAX stock #002831)(Lahvis and Bradfield, 1998). $AhR^{-/-}$ on the C57BL/6JRj background and wild type mice were housed and bred at Saint Antoine Research Center. $AhR^{-/-}$ and C57BL/6JRj at 5 weeks of age were fed *ad libitum* with a purified control diet (CD, Envigo TD.120508, Table S2) or high fat diet (HFD, 38% kcal fat, dominantly milk fat, Envigo TD.97222, Table S2) for 12 weeks. Ob/ob and wild-type mice at 6-7 weeks of age were fed *ad libitum* with standard chow diet (R03, SAFE, Augy, France) for 12 weeks. 6-week-old male Wistar were purchased from Janvier (France), used

1 week after receipt and fed with either standard chow diet or HFD with 45% of energy from lipids and 17% of energy from sucrose. Animals were weighed weekly, and weekly food consumption was measured in each cage. Except when *in-vivo* permeability experiments were performed, all animals were fasted for 6 hours prior to sacrifice and then anesthetized using isoflurane. Animals were euthanized by cervical dislocation, and appropriate tissues were harvested. All experiments were performed in accordance with the Comite d'Ethique en Experimentation Animale.

Metabolic syndrome cohort. All human subjects were selected from three cohorts of Paris Hospitals (Paris, France) and provided informed consent. None of the subjects had received antibiotics during the three months before sampling. Approval for human studies was obtained from the local ethics committees (Comité de Protection des Personnes Ile-de-France IV, IRB 00003835 Suivitheque study; registration number 2012/05NICB and Dispo cohort, registration number 2016/34 NICB; Comité de Protection des Personnes Ile-de-France III, Mabac cohort, registration number S.C. 3218).

METHOD DETAILS

Animal Treatments. For the AhR agonist treatments, mice were injected i.p. with 6-formylindolo(3,2-b)carbazole (Ficz, Enzo Life Sciences, 1 µg/mouse) or vehicle (dimethyl sulfoxide [DMSO]) once per week for 12 weeks. For the treatments with bacteria containing strong AhR activity, mice were gavaged daily with 10^9 CFU of *L. reuteri* CNCM I-5022 or vehicle (MRS broth supplemented with 0.05% L-cysteine and 15% glycerol) for 12 weeks.

Fecal microbiota transplantation. Fresh stool samples from CD-fed or HFD-fed mice (9-week-old males) were immediately transferred to an anaerobic chamber, in which the stool samples were suspended and diluted in LYHBHI (Brain-heart infusion) medium (BD Difco, Le Pont De Claix, France) supplemented with cellobiose (1 mg/ml; Sigma-Aldrich, St Louis, MO, USA), maltose (1 mg/ml; Sigma-Aldrich), and cysteine (0.5 mg/ml; Sigma-Aldrich). These fecal suspensions were used to inoculate mice. WT germ-free mice (4- to 5 week-old females) were randomly assigned to two groups and inoculated via oral gavage with 400 µl of fecal suspension (1:100) from the CD-fed or HFD-fed mice and maintained in separate isolators. All experiments in CD→GF and HFD→GF mice were performed three weeks after inoculation.

Measurement of AhR activity. The AhR activity of human and animal stool samples was measured using a luciferase reporter assay method, as described previously (Lamas et al., 2016). Briefly, H1L1.1c2 cells, which contained the dioxin response element-driven firefly luciferase reporter plasmid pGudLuc1.1, were seeded into a 96-well plate and stimulated with human or animal stool samples for 24 h. Luciferase activity was measured using a luminometer, and the results were normalized on the basis of the negative luciferase activity of the control.

Metabolite measurements. The metabolite concentrations of the stool samples were quantified as previously described (Lamas et al., 2016). Briefly, L-tryptophan and L-kynurenine were measured via HPLC using a colorimetric electrode assay (ESA

Coultronics). The indole derivatives were quantified by liquid chromatography coupled to mass spectrometry, using a Waters ACQUITY ultra performance liquid chromatography system (Garner et al., 2007). IDO activity was assessed by measurement of Kyn/Trp ratio.

16s rRNA gene sequencing. 16s rRNA gene sequencing of the fecal DNA samples (collected after 9 weeks of CD or HFD administration) was performed as previously described (Lamas et al., 2016). Briefly, the V3-V4 region was amplified, and sequencing was performed on an Illumina MiSeq platform (GenoScreen, Lille, France). Raw paired-end reads were subjected to the following process: (1) quality-filtering using the PRINSEQ-lite PERL script by truncating the bases from the 3′ end that did not exhibit a quality below 30, on the basis of the Phred algorithm; (2) paired-end read assembly using FLASH (fast length adjustment of short reads to improve genome assemblies) (Schmieder, R. & Edwards, R. Quality control and preprocessing of metagenomic datasets (Schmieder and Edwards, 2011) with a minimum overlap of 30 bases and a 97% overlap identity; and (3) search and removal of both forward and reverse primer sequences using CutAdapt, with no mismatches allowed in the primer sequences. Assembled sequences for which perfect forward and reverse primers were not found were eliminated. Sequencing data were analyzed using the quantitative insights into microbial ecology (QIIME 1.9.1) software package. The sequences were assigned to OTUs using the UCLUST algorithm (Edgar, 2010) with a 97% threshold of pairwise identity and classified taxonomically using the Greengenes reference database (McDonald et al., 2012). Rarefaction was performed (13,000 sequences per sample) and used to compare the abundance of the OTUs across samples. The alpha diversity was estimated using both the richness and evenness indexes

(Chao1, Shannon or number of observed species). The beta diversity was measured by using the Bray Curtis distance matrix and was used to build the PCoA. The linear discriminant analysis (LDA) effect size (LEfSe) algorithm was used to identify taxa that were specific to the diet or treatment (Segata et al., 2011).

Oral glucose tolerance test. OGGT was performed 3-7 days before sacrifice. Mice were fasted by removal of the food and bedding 1 hour before the onset of the light cycle. After 6 hours of fasting, a glucose solution (1 g/kg for ob/ob mice; 2 g/kg for all other mice) was administered by oral gavage. Blood glucose levels at time 0 (fasting glucose, taken before glucose gavage) and 15, 30, 60 and 120 min after glucose gavage were analyzed using a OneTouch glucometer (Roche). The glucose level was plotted relative to time, and the AUC was calculated according to the trapezoidal rule. The plasma insulin concentrations (collected in EDTA-coated tubes) at times 0 (fasting insulin) and 30 were analyzed from tail vein blood (collected in EDTA-coated tubes) by using an Ultra Sensitive Mouse Insulin ELISA Kit (Alpco). HOMA-IR was calculated according to the following formula: fasting glucose (nmol/L) x fasting insulin (microU/L)/22.5.

Intraperitoneal insulin tolerance test. ITT was performed 3-7 days before sacrifice. Mice were fasted by removal of the food and bedding 1 hour before the onset of the light cycle. After 6 hours of fasting, an insulin solution (0.5 U/kg) was administered intraperitoneally. Blood glucose levels at time 0 (fasting glucose, taken before glucose gavage) and at 15, 30, 60 and 120 min after the insulin challenge were analyzed using a OneTouch glucometer

(Roche). The glucose levels were plotted relative to time, and the AUC was calculated according to the trapezoidal rule.

Measurements of plasma parameters. Blood samples were collected in heparin-coated tubes via cardiac puncture and centrifuged. The plasma samples were then stored at -80°C until further analysis. Measurements of plasma cholesterol, triglycerides, high-density lipoprotein (HDL), aspartate transaminase (AST) and alanine transaminase (ALT) were performed by using the Biochemistry Platform (CRI, UMR 1149, Paris) with an Olympus AU400 Chemistry Analyzer.

Liver histology and hepatic triglyceride measurement. A slice of the left lobe of the liver was fixed in 4% PFA for 48 h and then transferred to ethanol, fixed in paraffin, trimmed, processed, sectioned into slices that were approximately 3 μm thick, mounted on a glass slide and stained with H&E. Hepatic lipids were evaluated and quantified blindly by using the ImageJ software as previously described(Crane et al., 2015; Schneider et al., 2012).

In vivo intestinal permeability and plasma sCD14 measurements. *In vivo* assays of intestinal barrier function were performed with the fluorescein-conjugated dextran (FITC-dextran, 4 kDA) method, as previously described (Laval et al., 2015). Briefly, on the day of sacrifice, FITC-dextran (0.6 mg/g of body weight) was administered to the mice by oral gavage, and 3 h later, blood samples were collected in heparin-coated tubes. The fluorescence intensity of the plasma was measured using a microplate reader (Tecan). The

plasma concentrations of soluble CD14 (sCD14) were measured using a CD14 ELISA kit (R&D) per the manufacturer's instructions.

Intestinal permeability measurements in Ussing chambers. Segments of the colon, mid-jejunum and distal ileum were cut along the mesenteric border and mounted in Ussing chambers (Physiological instruments), and 0.2-0.3 cm^2 of the tissue area was exposed to 2.5 mL of circulating oxygenated Kreb's bicarbonate buffer containing 5 mM KCl, 114 mM NaCl, 2.15 mM CaCl$_2$, 1.10 mM MgCl$_2$, 25 mM Na$_2$HCO$_3$, 1.65 mM Na$_2$HPO$_4$ and 0.3 mM NaH$_2$PO$_4$ and maintained at 37°C. Additionally, glucose (10 mM) was added to the serosal buffer as a source of energy and osmotically balanced by mannitol (10 mM) in the mucosal buffer. Fluorescein-labeled lipopolysaccharide (F-LPS; 80 µg/mL; Sigma-Aldrich) was used as a probe to assess macromolecular permeability. Additionally, antonia red-labeled dextran (ARD4; 400 µg/mL; molecular weight, 4000 Da; TdB) and fluorescein-labeled sulfonic acid (FS4; 40 µg/mL; molecular weight, 400 Da; TdB) were simultaneously used to assess paracellular and transcellular permeability. All probes were added to the luminal buffer once equilibrium was reached (10-15 min after mounting the tissues in the chamber). Serosal samples (200 □L) were obtained at 30-min intervals for 2 h and replaced with fresh buffer to maintain constant volume. The fluorescence intensity of the serosal samples was measured using a microplate reader (Tecan), and the concentrations of the probes were calculated from a standard curve. The flux of probes from the mucosa to the serosa was calculated as the average value of two consecutive stable flux periods (60–90 and 90–120 min) and expressed as ng/cm^2/h.

Monolayer Preparation and TEER measurement. Caco-2 cells were grown on Transwell semipermeable filter supports (12-mm diameter wells, polystyrene membranes with 0.4-mm pores, Costar-Corning) that were seeded at 1×10^5 cells per well; cells were used 18-20 days after confluence. TEER measurements were performed at time 0 (T0), which occurred before adding Ficz (175 nM) to both the apical and basal surfaces of the Transwells 3h before the cytokine stimulation, and at the end of the cytokine stimulation (time 36 h, T36). Cells were first stimulated with IFN-γ (10 ng/ml; R&D Systems) for 24 hours to promote expression of TNF-α receptors, followed then stimulated with TNF-α (2.5 ng/ml; R&D Systems) for 12 hours. Cytokines were added to only the basal compartment without manipulation of the apical compartment. Wells without Ficz and cytokines were used as controls. The TER data are presented as ratios: Ratio=(TER Treatment Time 36/TER Treatment T0)/(TER Control T36/TER Control T0). To examine the flux of fluorescein isothiocyanate-labeled dextran (FD4; molecular weight, 4000 Da; TdB), monolayers were washed after stimulation with Hanks' balanced salt solution (HBSS) and transferred to fresh HBSS; 1 mg/ml of fluorescein isothiocyanate-dextran was added to the apical layer and incubated at 37°C. Samples were removed from the basal chamber after 120 min. Fluorescence of the basal samples was determined using a fluorescence plate reader (Tecan), and flux was calculated from a standard curve. Experiments were performed twice in triplicate or quadruplicate for a total of two independent experiments.

GLP-1 Secretion. GLP-1 secretion was assessed with an immunoassay from GLUTag (Drucker et al., 1994). Cells were seeded in 24-well plates at 2×10^5 cells per well and cultured for 2-3 days. On the day of the experiment, cells were washed twice with Krebs

Ringer solution containing 30 mM KCl, 120 mM NaCl, 0.5 mM $CaCl_2$, 0.25 mM $MgCl_2$, and 2.2 mM $NaHCO_3$ supplemented with 0.5% (wt/vol) BSA. Cells were stimulated with Forskolin (10 µM; Sigma-Aldrich) or Ficz (175 nM; Enzo Pharmaceuticals) in the presence or absence of AhR antagonist CH223191 (10 µM; Sigma-Aldrich) or vehicle (DMSO) for 2 h in Krebs Ringer solution. GLP-1 concentrations at 0 h and 2 h were measured using a total GLP-1 ELISA kit (Millipore), per the manufacturer's instructions. The GLP-1 concentrations were expressed as the difference at 2 h and 0 h divided by the total cell protein concentration. Experiments were performed twice in triplicate or quadruplicate for a total of two independent experiments.

Cytokine quantification. Single-cell suspensions from the mesenteric lymph nodes and spleens were isolated by smashing the cells in a 70-µm mesh; 1×10^6 cells were seeded into 24-well plates and stimulated with phorbol 12-myristate 13-acetate (PMA, 50 ng/mL; Sigma-Aldrich) and ionomycin (1 µM; Sigma Aldrich) for 48 h at 37°C. Supernatants were collected and used for the cytokine analysis. Cytokines were measured using individual ELISA kits (the Mabtech IFN-γ ELISA kits; and the eBioscience TNF-α ELISA kit).

Gene expression analysis using quantitative reverse-transcription PCR. Total RNA was isolated from different intestinal segments using an RNeasy Mini Kit, according to the manufacturer's instructions. Quantitative RT-PCR was performed using a Bio-Rad iScript cDNA Synthesis kit and then a Takyon SYBR Green PCR kit in a StepOnePlus apparatus (Applied Biosystems) with specific mouse oligonucleotides that have been described

previously (Lamas et al., 2016). qPCR data were analyzed using the $2^{-\Delta\Delta Ct}$ quantification method with mouse *gapdh* as the endogenous control.

Fecal bacterial quantification. Fecal DNA was extracted and bacterial abundance was quantified by qPCR as previously described (Lamas et al., 2016).

QUANTIFICATION AND STATISTICAL ANALYSIS

In each experiment, multiple mice were analyzed as biological replicates. No statistical methods were used to predetermine the sample size. Dot plots with a linear scale show the arithmetic mean. Bar graphs are expressed as the mean ± standard error of the mean (SEM). Except for the 16s rRNA results, GraphPad Prism version 7.0b was used for statistical analyses. The Kolmogorov-Smirnov test was used to verify that the entire data set was normally distributed. For data sets that failed normality tests, nonparametric tests were used to analyze significant differences. For comparisons between two groups, significance was determined using the two-tailed Student's t-test or nonparametric Mann-Whitney test. For comparisons among more than two groups, one way (ANOVA) followed by post hoc Bonferroni tests, nonparametric Kruskal-Wallis tests followed by post hoc Dunn's tests or two-way ANOVA corrected for multiple comparisons with a Bonferroni test were used. An F or Bartlett's test was performed to determine differences in variances for t-tests and ANOVAs, respectively. An unpaired Student's t-test with Welch's correction was applied when variances were not equal. Differences were noted as significant at $p \leq 0.05$.

DATA AND SOFTWARE AVAILABILITY

Sequencing data are deposited under accession number AF29742 in the NCBI Trace and Short-Read Archive and, for data shown in Figure S4B, in the European Nucleotide Archive under accession number PRJEB27333.

KEY RESOURCE TABLE

REAGENT or RESOURCE	SOURCE	IDENTIFIER
Bacterial Strains		
Lactobacillus reuteri		CNCM I-5022
Lactobacillus helveticus		CNRZ450
Chemicals, Peptides, and Recombinant Proteins		
Control Diet	Envigo	TD.120508
High Fat Diet	Envigo	TD.97222
Glucose	Sigma-Aldrich	G8270
EDTA-coated tubes	Sarstedt	16.444
Heparin-coated tubes	Sarstedt	41.1393.105
Phorbol 12-myristate 13-acetate	Sigma-Aldrich	P8139
Ionomycin calcium salt	Sigma-Aldrich	I0634
T-per tissues protein extraction reagent	Thermo Fisher	78510
BCA Protein Assay kit	Thermo Fisher	23252
FITC-dextran 4	TdB	FD4
Critical Commercial Assays		
Insulin Ultrasensitive ELISA kit	Alpco	80-INSMSU-E01
Legendplex Mouse Inflammation Panel	Biologend	740150
IL-6 ELISA kit	R&D	DY406-05
IFN-γ ELISA kit	Mabtech	3321-1H-6
IL-17a ELISA kit	Mabtech	3521-1H-6
TNF-α ELISA kit	Affymetrix eBioscience	88-7324-86
CD14 ELISA KIT	R&D	DY982
LCN2 ELISA kit	R&D	DY1857
Experimental Models: Organisms/Strains		
Mouse: C57BL/6JRj	Janvier	SC-C57J-M
Mouse: Ob/Ob	Janvier	
Mouse: AhR$^{-/-}$	JAX	#002831

Figure 1

Click here to download Figure Final Figure 1.tif ±
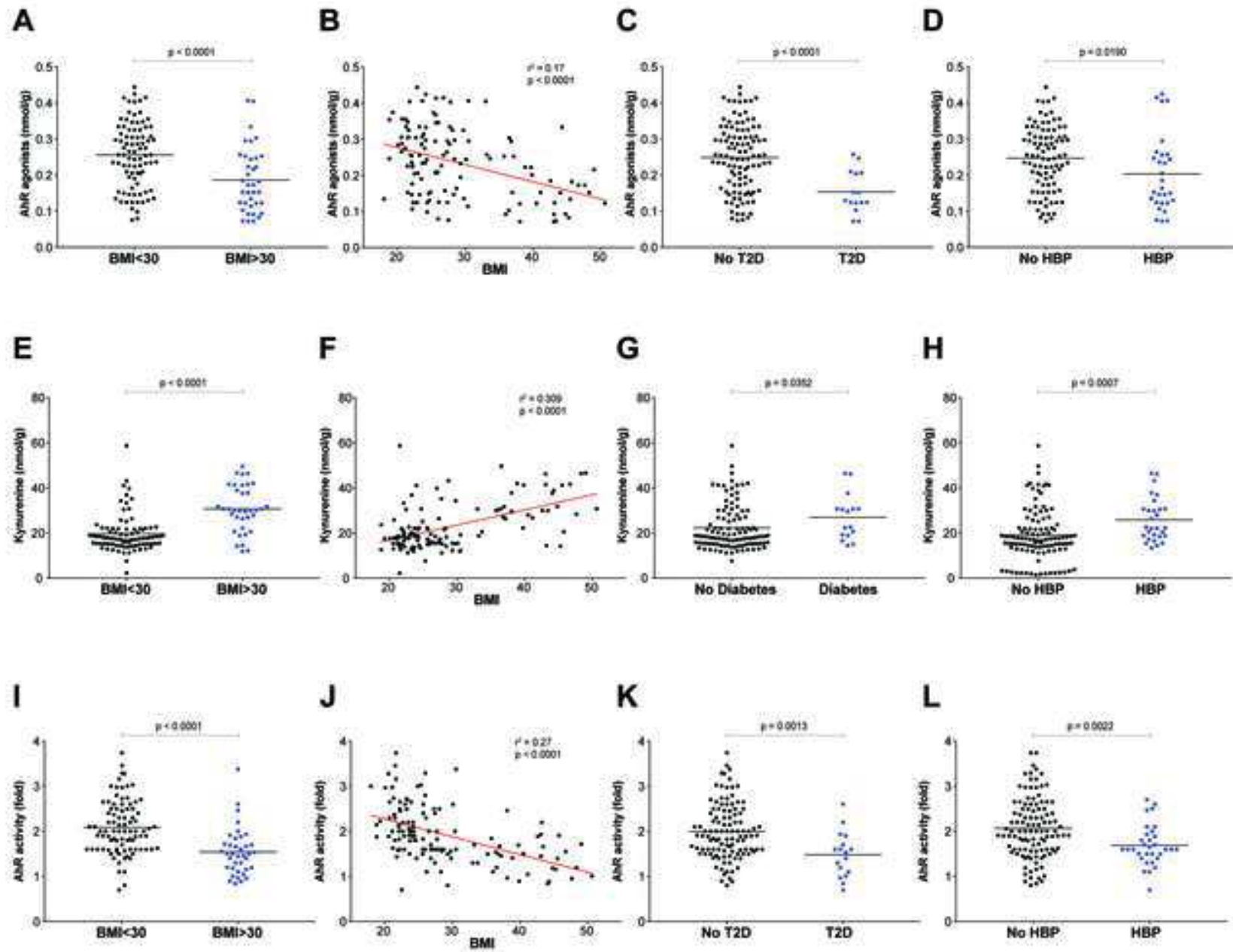
Figure 1

Figure 2
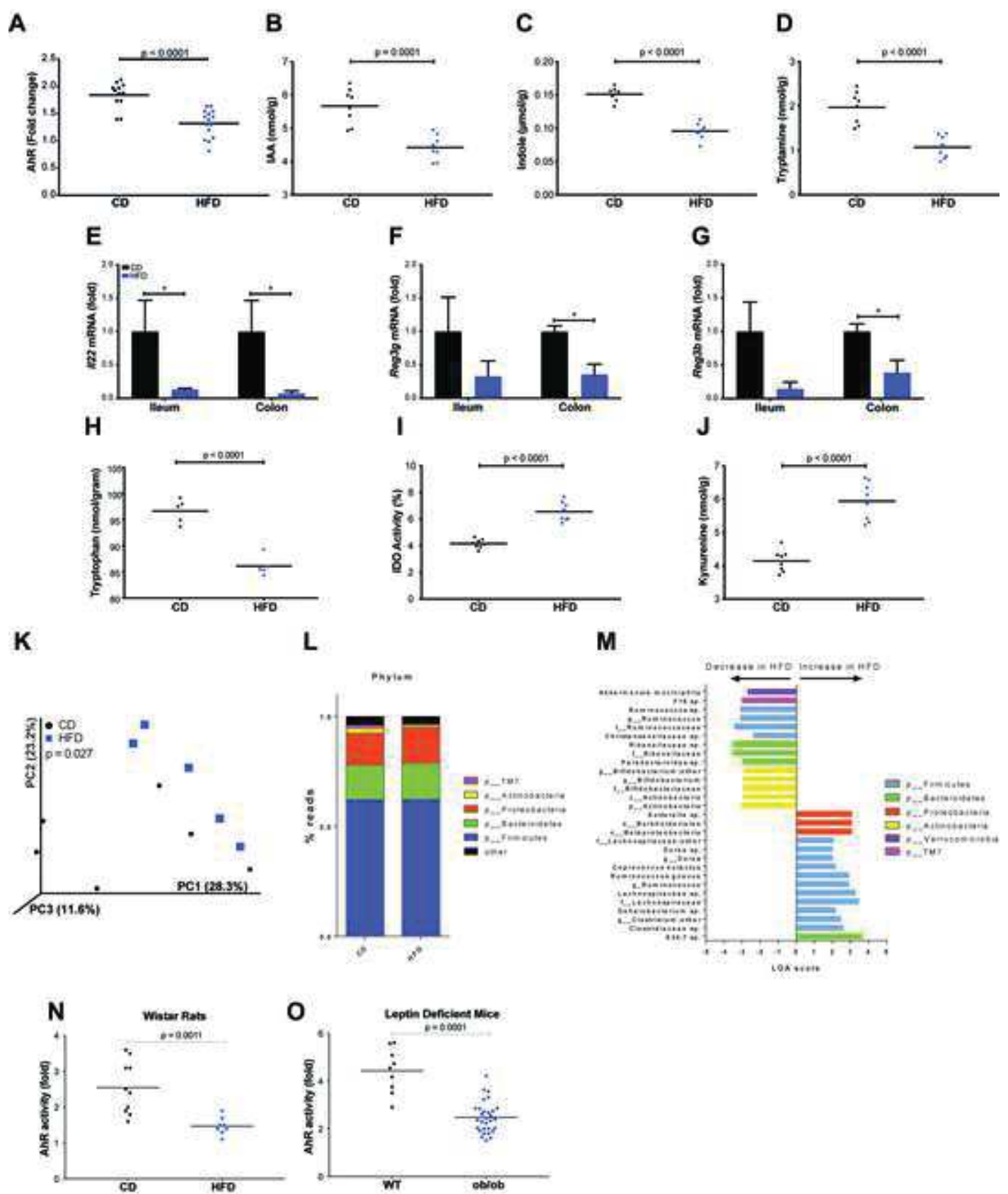
Figure 2

Figure 3
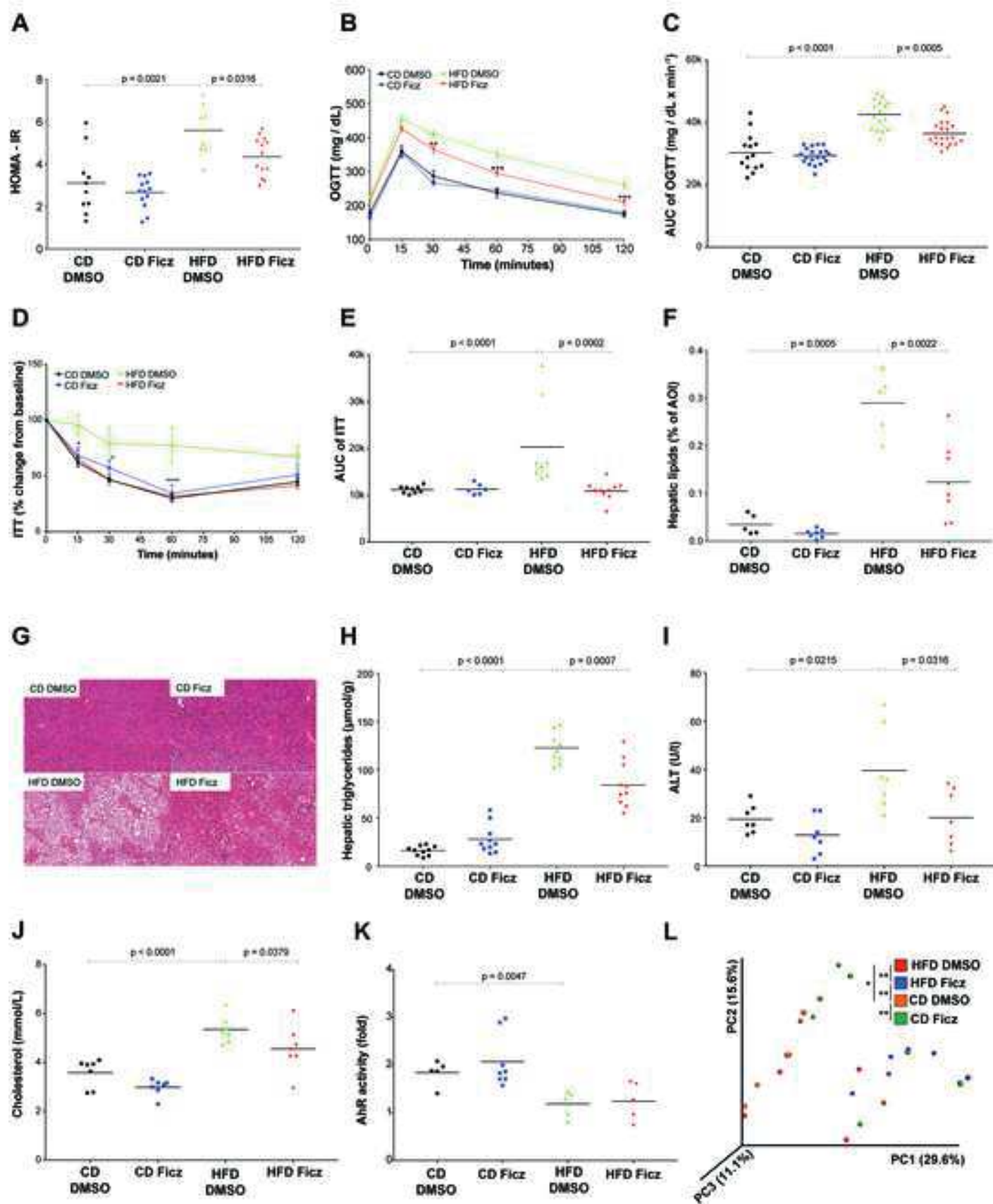
Figure 3
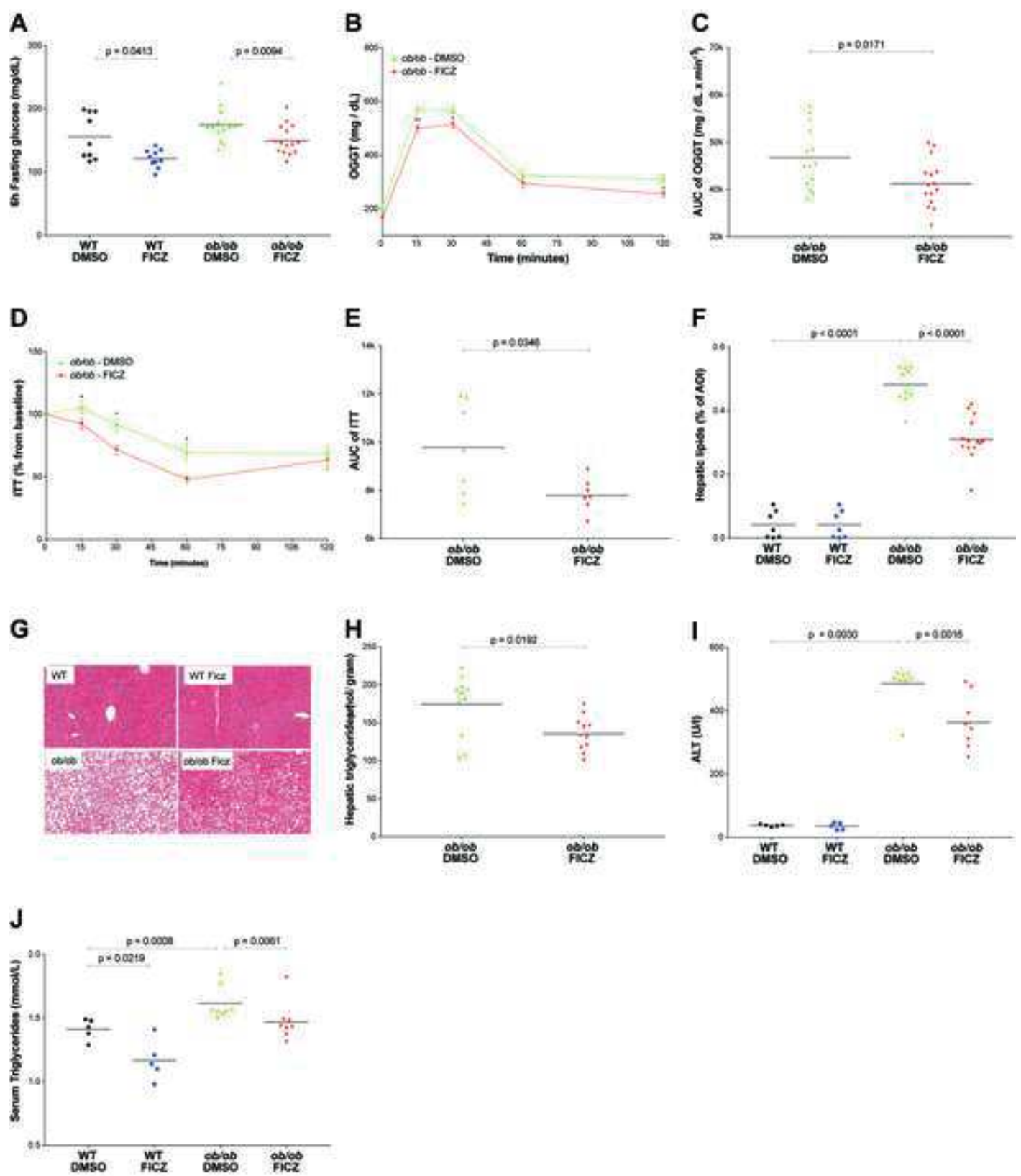
Figure 4

Figure 4
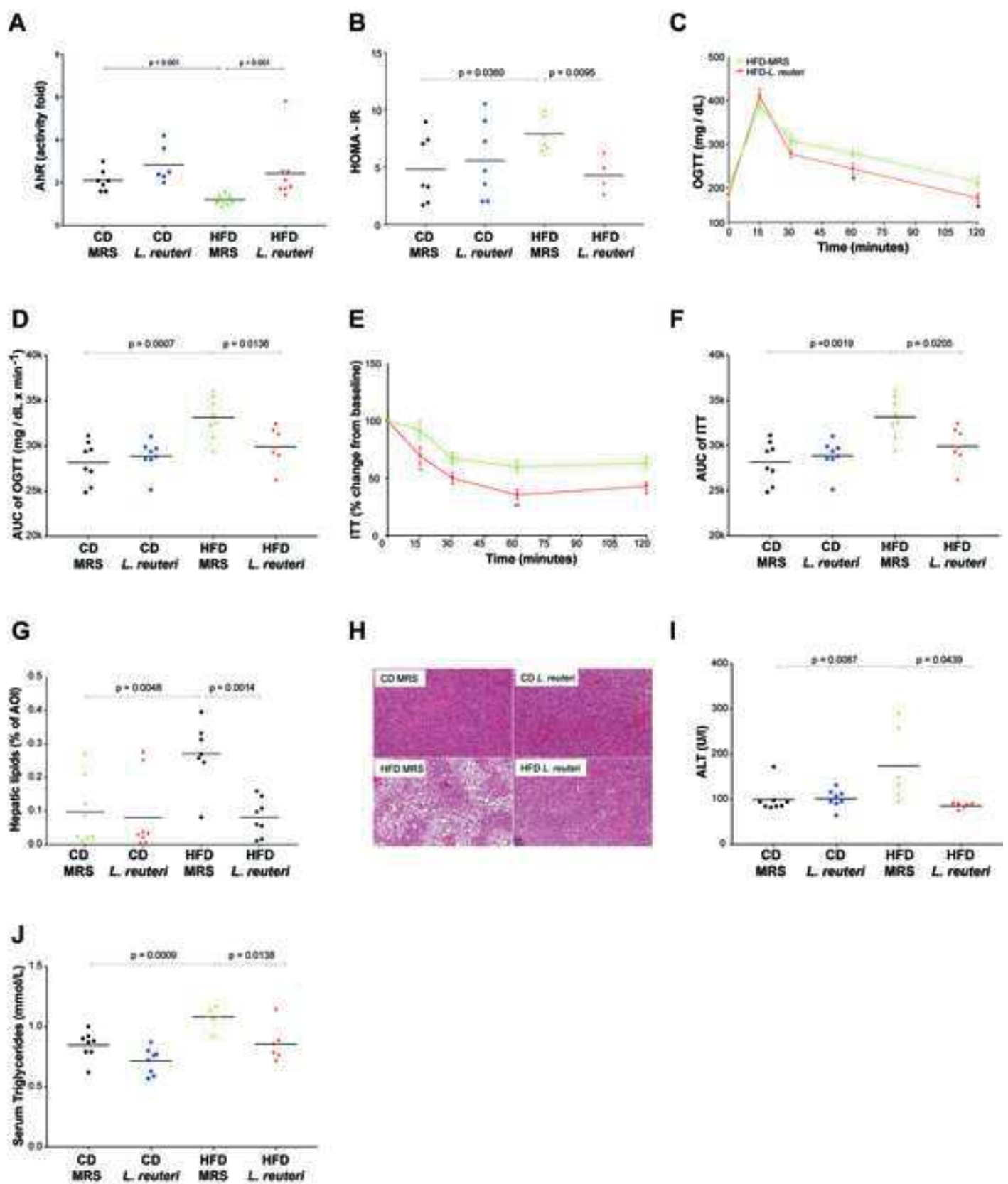
Figure 5

Figure 6
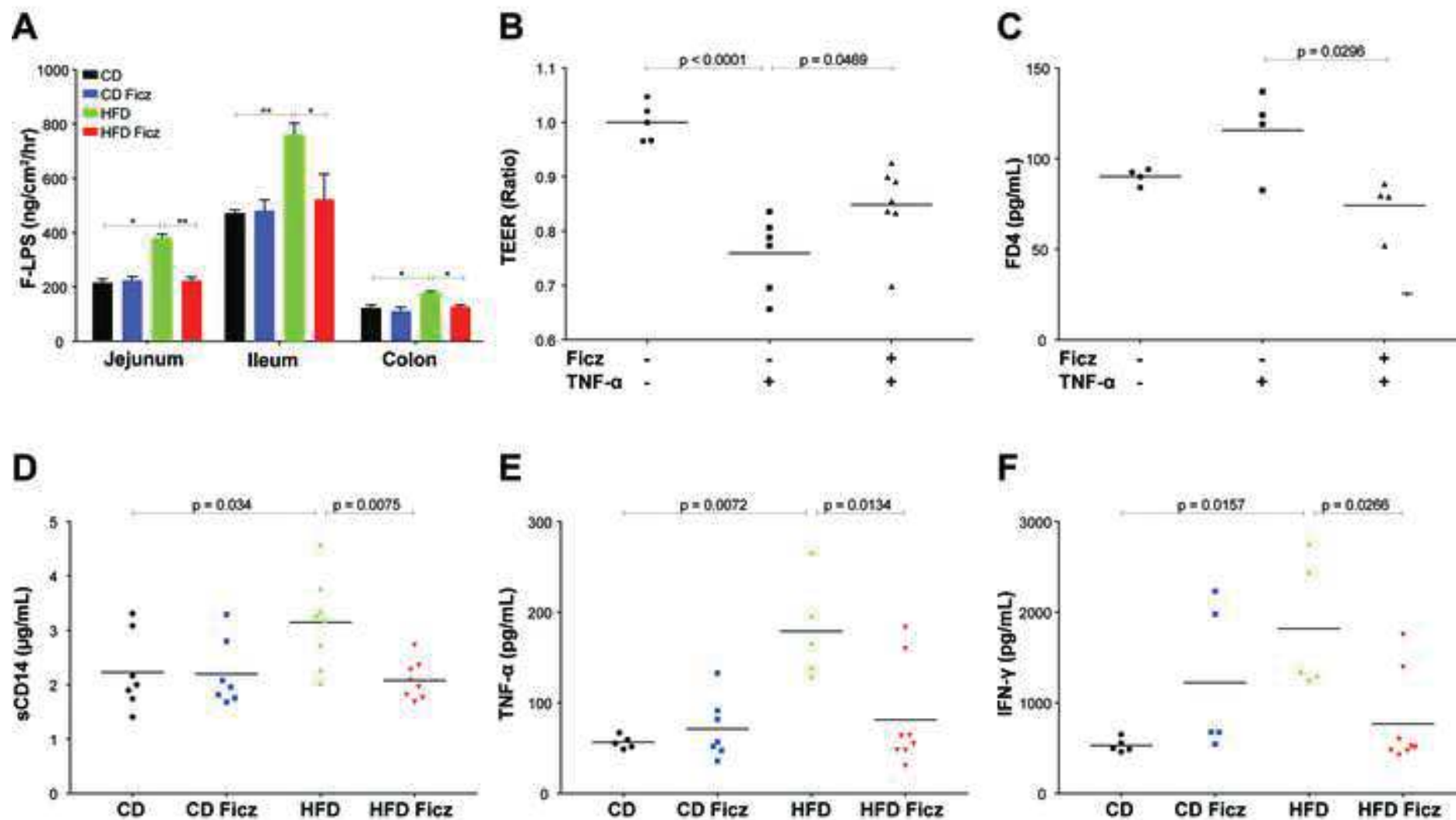
Figure 6
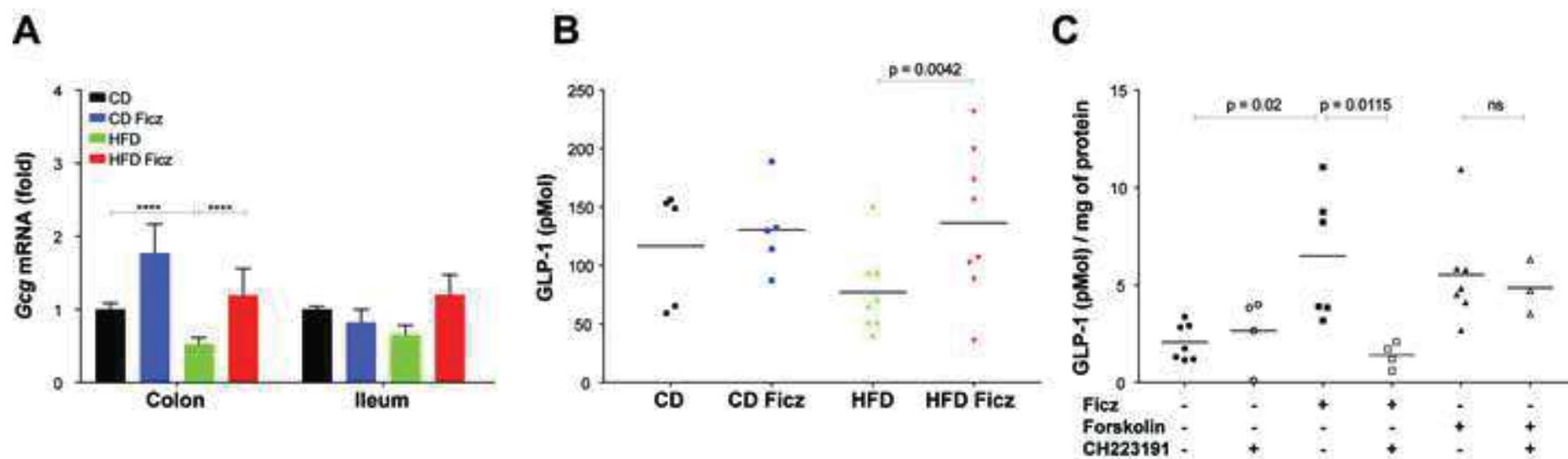
Figure 7

Figure 7

Supplemental Figure 1
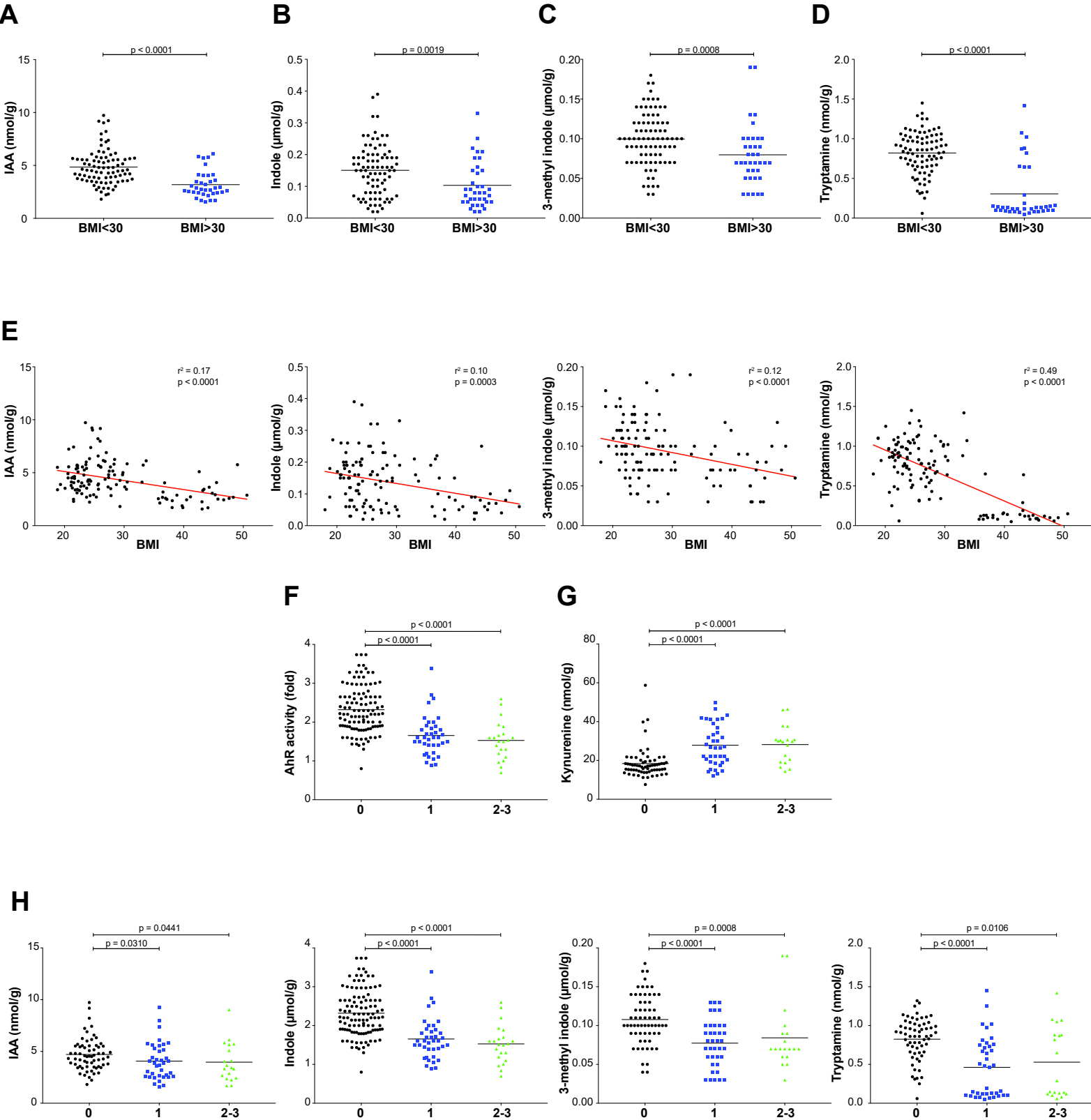
Figure S1 (Related to Figure 1). The microbiota of obese individuals displays lower levels of microbiota-derived AhR agonists. Concentrations of (A) IAA, (B) indole, (C) 3-methylindole and (D) tryptamine from feces of individuals with low and high BMIs. (E) Spearman correlation of the stool AhR agonist concentration and BMI. Stools from individuals possessing one or more metabolic risk factors showed lower (F) AhR activity, higher (G) kynurenine and increased levels of (H) AhR agonists. For AhR reporter assay, data was available in the whole population (n=127). For AhR agonist dosage, results were not available in 4 patients (3 with BMI>30 and 1 with BMI<30). Statistical comparisons were performed by normality testing using Kolmogorov-Smirnov tests and subsequent ANOVAs or Kruskal-Wallis tests with Bonferroni or Dunn's *post hoc* tests.

Supplemental Figure 2
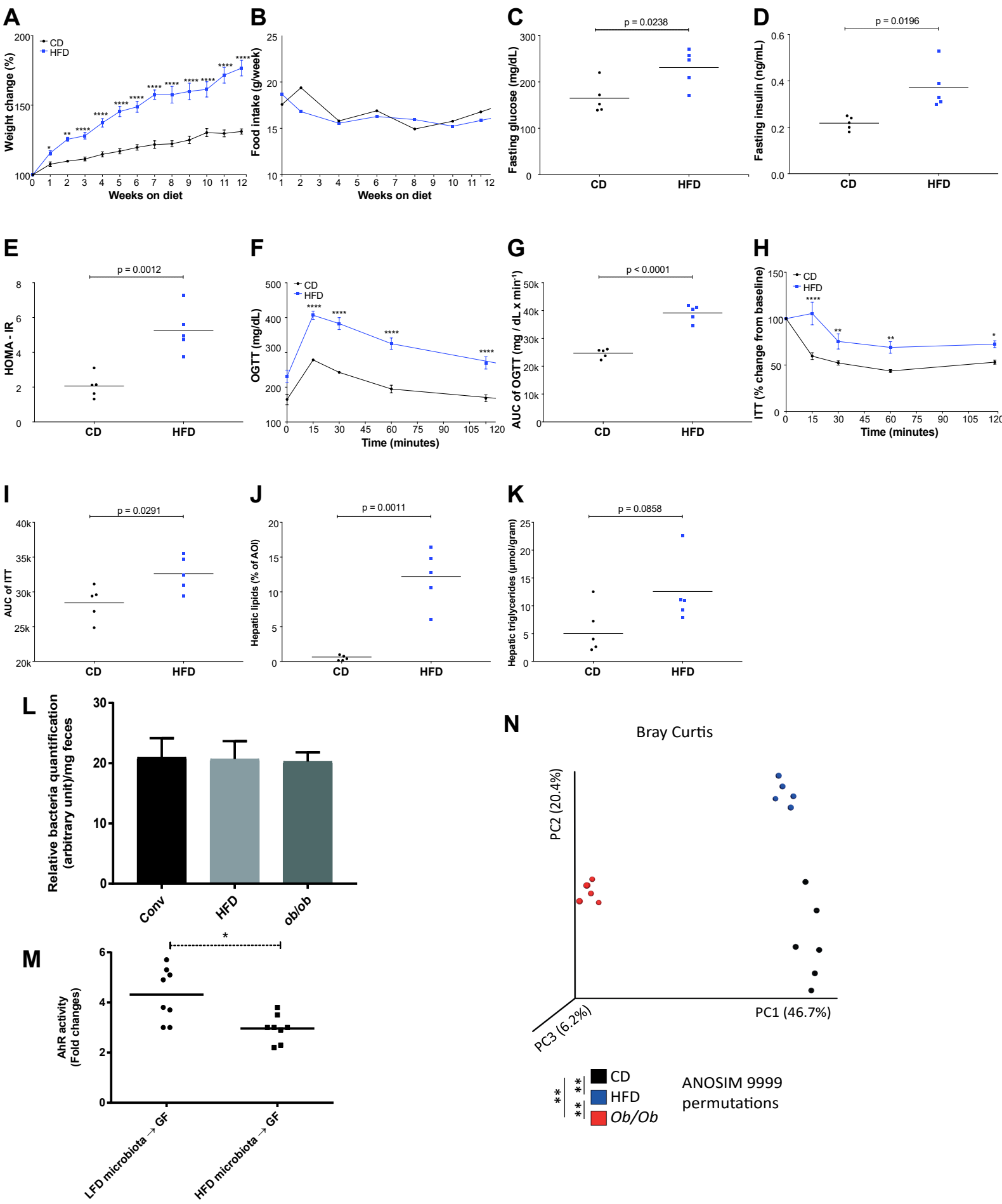
**Figure S2 (Related to Figure 2).** HFD-fed mice show defective tryptophan metabolism by the microbiota and exhibit metabolic host dysfunctions. (A) Body weight gain and (B) weekly food intake of mice. (C) Blood glucose, (D) insulin, and (E) HOMA-IR after 6 h of fasting. (F) Blood glucose levels before and after the OGTTs. (G) The area under the curve (AUC) of the OGTT. (H) Blood glucose levels, expressed as change from baseline, before and after the ITTs. (I) The AUC of the ITT. (J) Lipid area, calculated as the % AOI, in the H&E-stained liver cross-sections. (K) Liver triglycerides after 6 h of food deprivation. (L) No difference in bacterial abundance in CD-fed, HFD-diet and ob/ob mice using qPCR (n=12/group). (M) Fecal AhR agonist activity in germ-free mice colonized with HFD-fed or CD-fed mice microbiota. (N) Principal coordinate analysis (PCoA) plot of Bray Curtis distances of the fecal microbiota of the CD-fed, HFD-fed and ob/ob mice (n=5-6/group, Anosim test, 9999 permutations). (*$p<0.05$, **$p<0.01$, ****$p<0.0001$, n=5/group). Statistical comparisons were carried out by normality testing using Kolmogorov-Smirnov tests and subsequent unpaired *t*-tests or Mann-Whitney tests.

Supplemental Figure 3
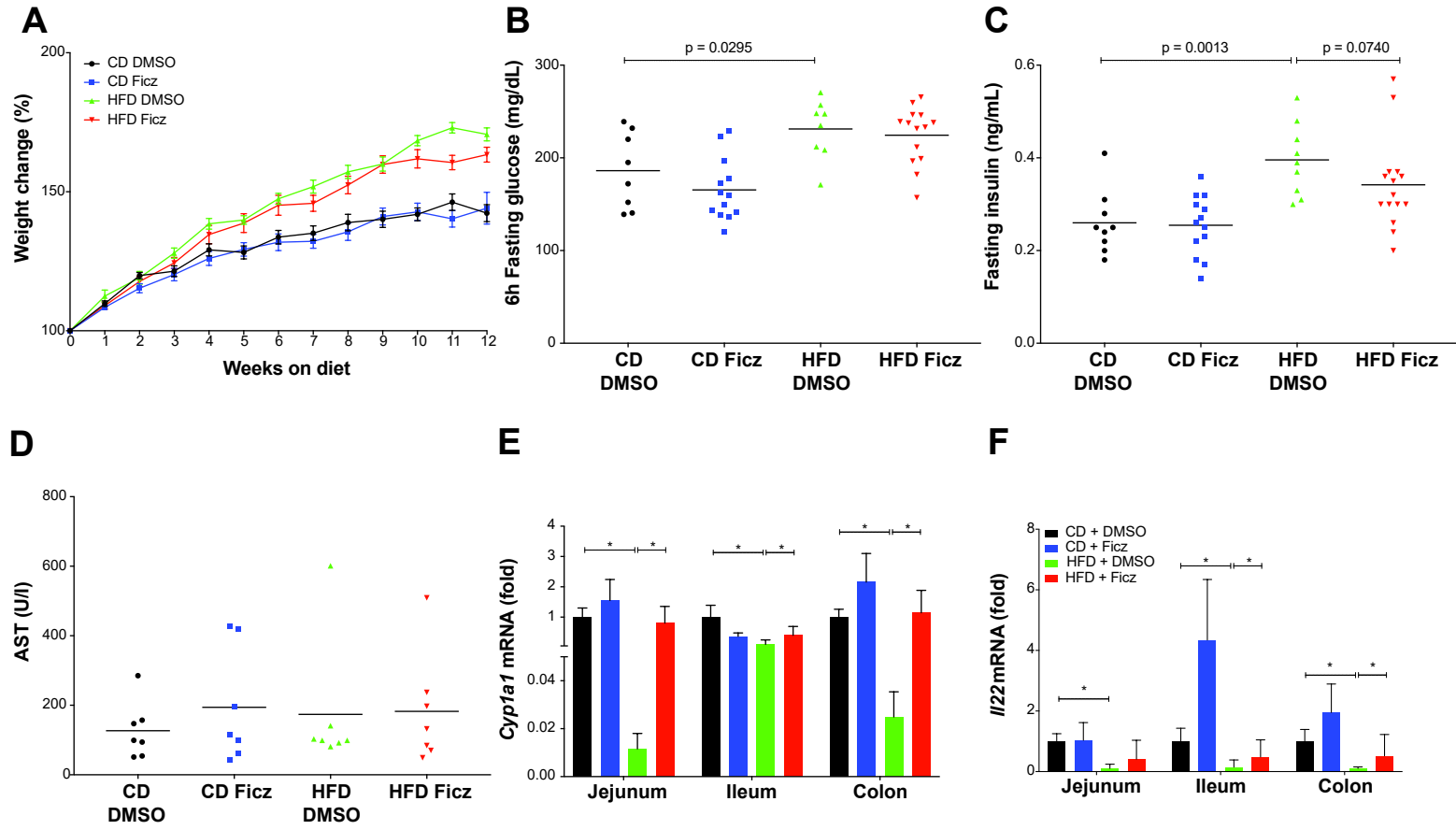
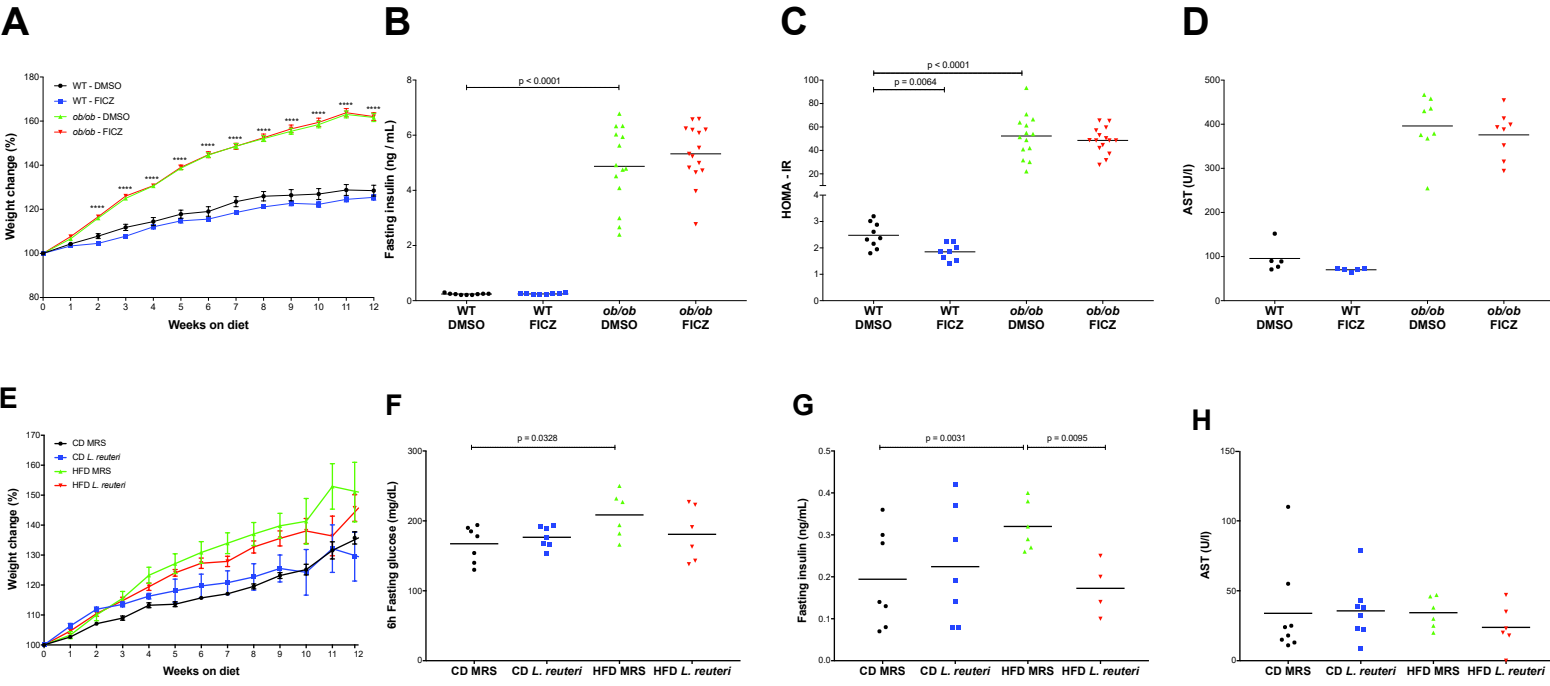**Figure S3 (Related to Figure 3).** Treatment with AhR agonist Ficz attenuates HFD-induced metabolic dysfunction. (A) Body weight gain (n=10/group). (B) Blood glucose and (C) insulin after 6 h of fasting. Concentrations of (D) aspartate transaminase (AST). Transcript expression of (E) *Cyp1a1* and (F) *Il22* in different intestinal segments of the indicated mice (*$p<0.05$, n=5-12/group). For all data, statistical comparisons were carried out by normality testing using the Kolmogorov-Smirnov test and subsequent ANOVAs or Kruskal-Wallis tests with Bonferroni or Dunn's *post hoc* tests (*$p<0.05$,**$p<0.01$, ***$p<0.001$).

Supplemental Figure 4
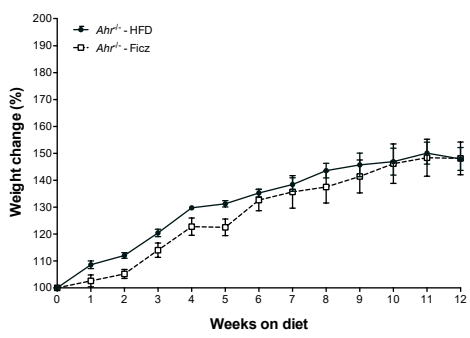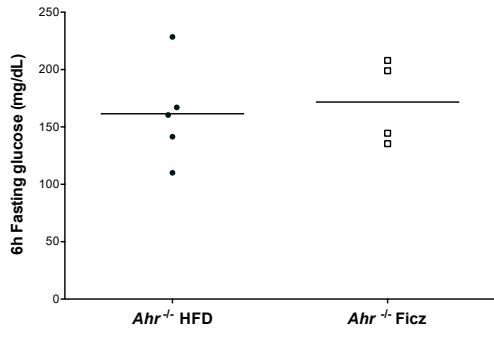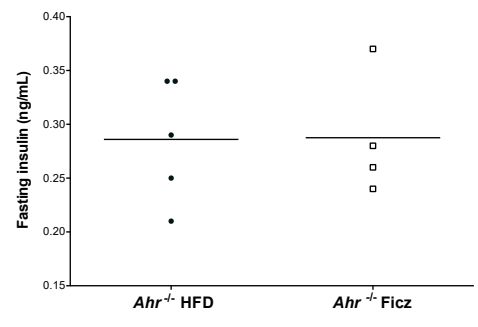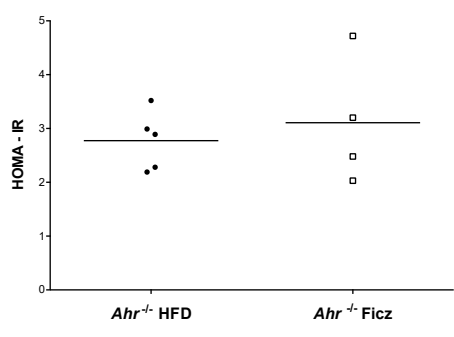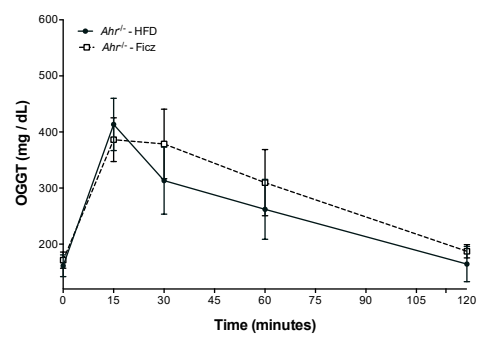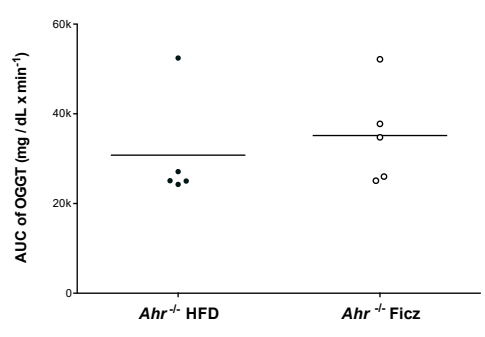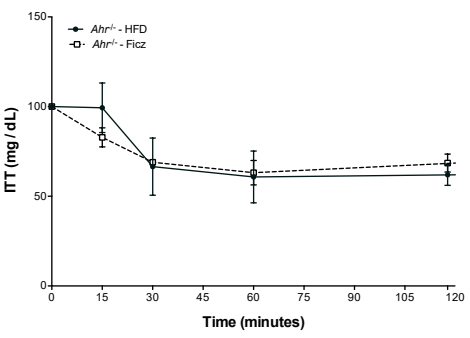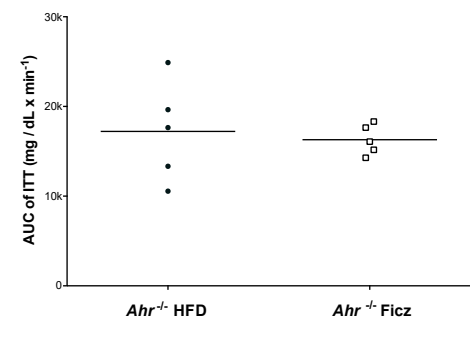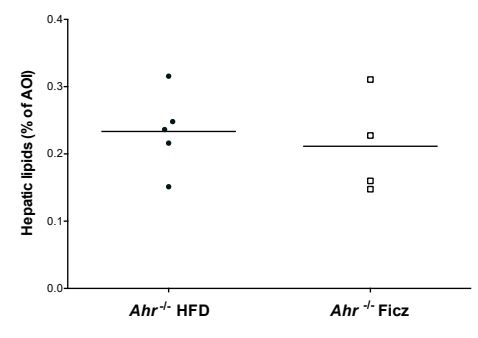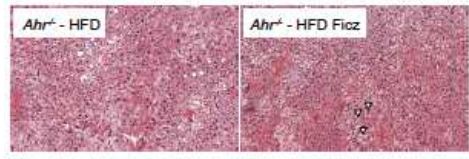
Figure S4 (Related to Figure 3). Treatment with AhR agonist Ficz failed to decrease features of metabolic syndrome in *AhR*$^{-/-}$ mice. (A) Body weight gain (n=4-5/group). (B) Glucose, (C) insulin and (D) HOMA-IR after 6 h of fasting. (E) The glucose levels before and after the OGTT (**p<0.01 n=4-5/group). (F) The AUC of the OGTT. (G) Blood glucose levels before and after the ITTs (*p<0.05 vs HFD, n=4-5/group). (H) The AUC of the ITT. (I) The lipid area in the liver cross-sections of indicated mice. (J) Representative pictures of H&E–stained liver sections from indicated mice. Statistical comparisons were performed by normality testing using Kolmogorov-Smirnov tests and subsequent unpaired *t*-tests or Mann-Whitney tests.

Supplemental Figure 5

Figure S5 (Related to Figures 4 &5). Treatment with an AhR agonist alleviates genetic-induced metabolic impairments and inoculation with high AhR ligand-producing bacteria attenuates HFD-induced metabolic syndrome. (A) Body weight gain (n=14-15/group). (B) Insulin after 6h of fasting. (C) HOMA-IR of indicated mice. (D) Concentrations of aspartate transaminase (AST). (E) Body weight gain (n=8/group). (F) Blood glucose and (G) insulin after 6 h of fasting. (H) Concentrations of aspartate transaminase (AST) in the sera of indicated mice. For all data, statistical comparisons were carried out by normality testing using the Kolmogorov-Smirnov test and subsequent ANOVAs or Kruskal-Wallis tests with Bonferroni or Dunn's *post hoc* tests ($*p<0.05, **p<0.01, ***p<0.001$).
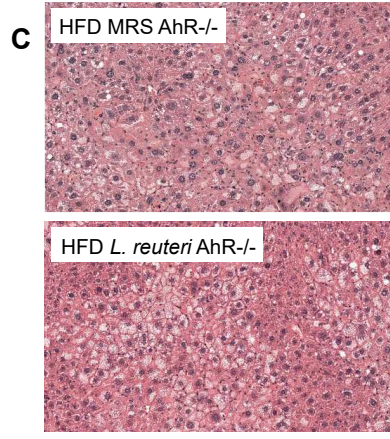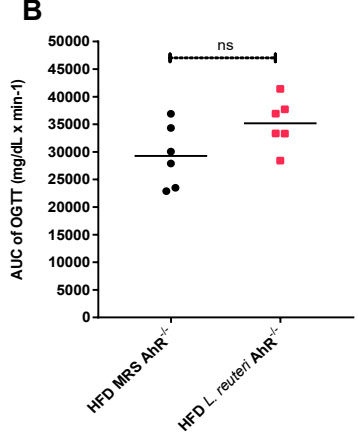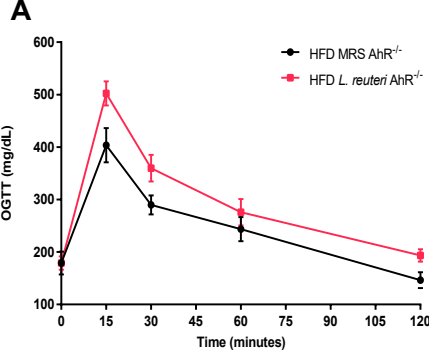
Supplemental Figure 6
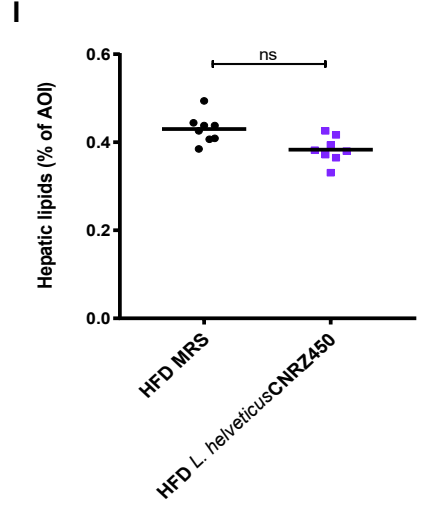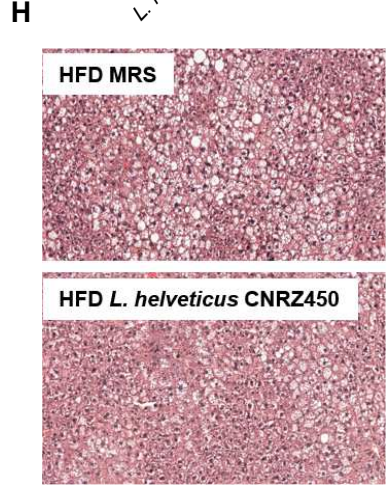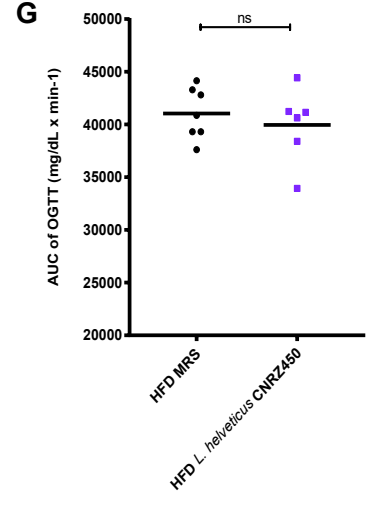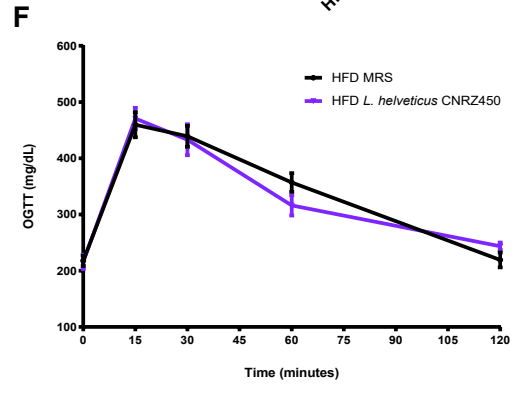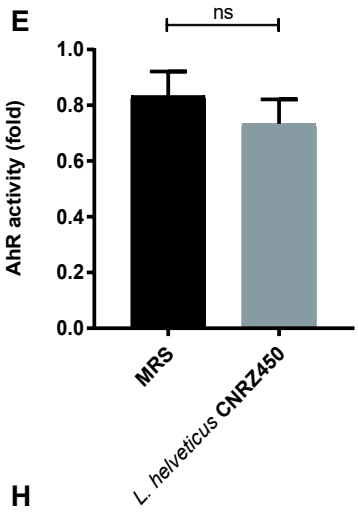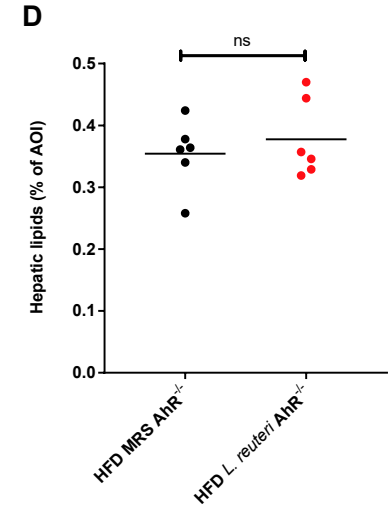
Figure S6 (Related to Figure 5). Beneficial effect of *L. reuteri* strain in HFD-induced metabolic syndrome is lost AhR$^{-/-}$ mice and *Lactobacillus* strain that does not exhibit AhR-ligand production does not improve metabolic syndrome. (A) Blood glucose levels before and after the OGTTs of AhR$^{-/-}$ mice supplemented with *L. reuteri* or vehicle. (B) The AUC of the OGTT. (C) Representative pictures of H&E–stained liver sections from indicated mice. (D) The lipid area in the liver cross-sections of indicated mice (n=6/group). (E) Quantification of AhR agonist activity of *L. helveticus* culture supernanant and control culture media MRS. (F) Blood glucose levels before and after the OGTTs of WT mice supplemented with *L. helveticus* or vehicle. (G) The AUC of the OGTT. (H) Representative pictures of H&E–stained liver sections from indicated mice. (I) The lipid area in the liver cross-sections of indicated mice (n=6-7/group). For all data, statistical comparisons were carried out by normality testing using the Kolmogorov-Smirnov test and subsequent unpaired t-tests or Mann-Whitney test.

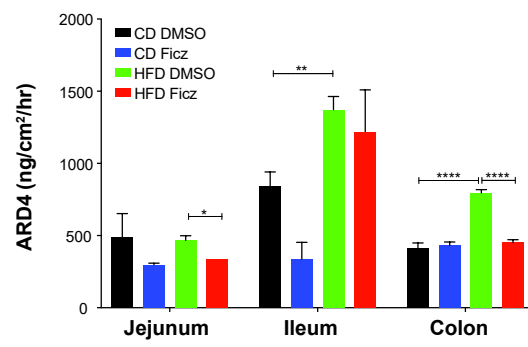# Supplemental Figure 7

A
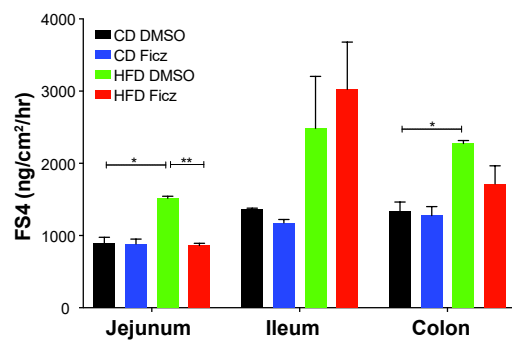
B

Figure S7 (Related to Figure 6). Treatment with an AhR agonist improves HFD-induced intestinal barrier dysfunction. Translocation of (A) sulfonic acid (FS4) and (B) dextran (ARD4) across the mucosa in different intestinal segments mounted in an Ussing chamber (*p<0.05, **p<0.01, ****p<0.0001, n=6-12/group). For all data, statistical comparisons were carried out by first testing normality using Kolmogorov-Smirnov tests and then performing ANOVAs or Kruskal-Wallis tests with Bonferroni or Dunn's *post hoc* tests.

Table S1. Clinical subjects information (Related to Figure 1).

	Whole population	Subjects with Metabolic Syndrome	Healthy controls
n	127	92	35
Male gender (n,%)	58 (45.7)	43 (46.8)	15 (42.9)
Age (mean, SD)	51 (17)	58 (14)	35 (13)
BMI (mean, SD)	29 (8)	31 (8)	23 (3)
BMI>30 (n, %)	38 (30)	37 (40)	1 (3)
High blood pressure (n,%)	32 (25)	32 (35)	0
Diabetes (n, %)	17 (13)	17 (18)	0

Table S2. Diets composition (Related to Figures 2, 3, 5, 6, 7).

	Control Diet		High Fat Diet	
Composition	Corn starch, maltodextrin, casein powder, sucrose, soybean oil, calcium carbonate, mono-potassium phosphate, sodium chloride, potassium sulfate, magnesium oxide		Sucrose, casein powder, butter, maltodextrin, corn starch, mineral dicalcium phosphate, calcium carbonate, sodium chloride, potassium sulphate, magnesium oxide	
Nutritional additives	E672 Vitamin A	19800 (I.U.)	E672 Vitamin A	19800 (I.U.)
	E671 Vitamin D3	2200 (I.U.)	E671 Vitamin D3	2200 (I.U.)
	E1 Fe	40.2 (mg)	E1 Fe	40 (mg)
	E5 Mn	10.5 (mg)	E5 Mn	58.5 (mg)
	E6 Zn	33.5 (mg)	E6 Zn	32.5 (mg)
	E4 Cu	6 (mg)	E4 Cu	5.80 (mg)
	E2 I	0.21 (mg)	E2 I	0.21 (mg)
	E8 Se	0.15 (mg)	E8 Se	0.15 (mg)
	E7 Mo	0.15 (mg)		
Analytical constituents (% kcal from)	Protein	14	Protein	16
	Fat	10.3	Fat	38
	Carbohydrate	75.9	Carbohydrate	47